

Breakdown of conventional hydrodynamics for smectic-*A*, hexatic-*B*, and cholesteric liquid crystals

Gene F. Mazenko, Sriram Ramaswamy,* and John Toner†

The James Franck Institute and the Department of Physics, The University of Chicago, Chicago, Illinois 60637

(Received 12 April 1983)

We present a detailed analysis of anharmonic effects on the viscous and elastic properties of various systems with one-dimensional order. We show that the nonlinear coupling of the velocity field to thermally excited undulation modes causes four of the five viscosities in these uniaxial systems (including one, η_2 , governing shear flow in the layers) to diverge as $1/\omega$ when measured at small frequencies ω . As a result, sound attenuations scale as ω , rather than ω^2 as in most materials. A simple algebraic relation between the divergent parts of three of the viscosities is derived. We argue that the divergence in η_2 leads to strongly non-Newtonian flow in the liquid layers of these materials. The calculations here extend the previous work of the authors to include an analysis of irreducible graphs to all orders in perturbation theory in the temperature. Some new results on the nonlinear elastic theory of these systems are also obtained, extending earlier work by Grinstein and Pelcovits. The existing experimental evidence for our predictions is discussed, and additional experiments are suggested.

I. INTRODUCTION

In a previous paper¹ we reported that certain viscosities in smectic-*A* liquid crystals diverge as $1/\omega$ at small frequencies ω . In this paper we describe the details of our calculation and, in addition, present several new results for both the dynamic and static² properties of these materials. We will also show that our results apply without any modification to cholesteric³ and hexatic-*B* liquid crystals⁴ as well. The unifying features of these systems, and the ultimate cause of the divergences, is their “layering,” or “one-dimensional solidification.”⁵ Each exhibits a static, unidirectional spatial modulation (see Fig. 1) of some field (the density in smectics-*A* and hexatics-*B*; the molecular director in cholesterics). In smectics-*A*, this is the only type of ordering present, while the hexatics-*B* have sixfold orientational order⁴ as well. This additional ordering has no effect on the “undulation mode” depicted in Fig. 2, which is the principal thermally excited mode in these systems. Although the layering field in cholesterics is microscopically different from that in smectics, the hydrodynamic equations are nonetheless the same.^{3,6} It is the nonlinear interaction of externally applied stresses with these thermally excited modes, which cost very little energy and hence exist in great profusion in thermal equilibrium, that causes the viscosities to diverge.

In conventional three-dimensional materials (e.g., solids, liquids, gases, nematic liquid crystals, etc.), the viscosities may be taken to be independent of the wave vector and frequency of the excitations under consideration except near second-order phase transitions. The resultant description of dissipation in these systems becomes asymptotically exact⁶ in the limit of long wavelengths and low frequencies (the hydrodynamic limit). In contrast, our calculations show that over the entire smectic-*A*, hexatic-*B*, and cholesteric phases such a description breaks down. We must, instead, replace four of the five viscosities η_i ,

required by uniaxial symmetry,⁶ with strongly wave vector- and frequency-dependent quantities η_1 , η_2 , η_4 , and η_5 . These four viscosities are given in the small wave number \vec{q} and frequency ω limit by

$$\eta_i(\vec{q}, \omega) = \eta_i^0 + a_i I(\vec{q}, \omega), \quad (1.1)$$

where η_i^0 is a nondivergent background contribution to the viscosity,

$$I(\vec{q}, \omega) \sim \begin{cases} \omega^{-1}, & \omega \gg q_z (\kappa B / \rho_0)^{1/2} \\ q_z^{-1}, & \omega \ll q_z (\kappa B / \rho_0)^{1/2} \end{cases} \quad (1.2a)$$

$$(1.2b)$$

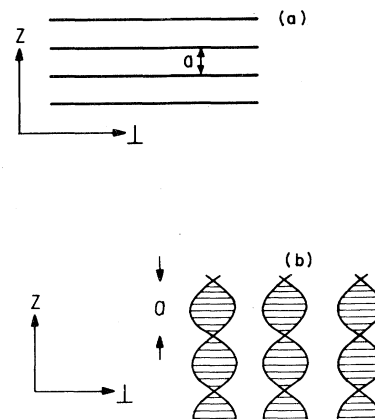


FIG. 1. (a) Vertical cross section of the ground state of smectics-*A*. Density is periodic with period $a \sim 20$ Å. Horizontal lines are surfaces of a given density. (b) Same as (a) for cholesteric liquid crystal. Spatially modulated quantity is now the molecular director \hat{n} which rotates at a constant spatial rate as one moves in the z direction with period $a \sim 4000$ Å. Surfaces of constant n (not shown) would also be horizontal planes.

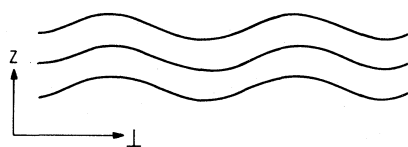


FIG. 2. Principal excitation in these systems: the undulation mode. Wavy lines are the new (perturbed) surfaces of constant density. Note that the displacement of the layers is a function only of the distance in the direction along the unperturbed layers.

The z axis is taken to be perpendicular to the layers, and B , ρ_0 , and the dimensionless parameter κ are defined in Table I. The phenomenological constants a_i in (1.1) obey the relation

$$a_1 a_4 = a_5^2 \quad (1.3)$$

and their numerical values are estimated in Table I. These quantities, as discussed in Sec. IV B, are not, strictly speaking, constants, but weakly diverging functions of wave number. Expressions for the a_i 's valid at low tem-

TABLE I. This table summarizes the various parameters appearing in the theory, provides an index to their defining equations (where appropriate) and gives estimates of their orders of magnitude for typical smectic- A and hexatic- B materials. Note that the elastic constant B is systematically larger for monolayer materials.

Parameter	Definition	Defining equation	Order of magnitude
Bare elastic constants			
A_0	Bulk modulus	(2.2)	5×10^{10} dyn/cm ² ^a
B_0	Dynamic layer compressibility	(2.2)	2×10^9 dyn/cm ² ^b (monolayer) 5×10^7 dyn/cm ² (bilayer)
K_1^0	Layer bending stiffness	(2.2)	5×10^{-7} dyn ^c
C_0	Layer density coupling	(2.2)	$B_0/5$ ^a
B'_0	Static layer compressibility $= B_0 - C_0^2/A_0$		B_0
Bare viscosities			
Bulk			
η_1^0	Layer-normal	(3.14)	1 cm ² /sec ^d
η_4^0	In-layer	(3.14)	1 cm ² /sec ^d
η_5^0	In-layer—layer-normal cross term	(3.14)	1 cm ² /sec ^d
Shear			
η_2^0	In-layer	(3.14)	0.1 cm ² /sec ^d
η_3^0	Layer-normal	(3.14)	0.1 cm ² /sec ^d
Lengths			
λ_0	$(K_1^0/B'_0)^{1/2}$ Layer spacing		20 Å Smectics: 20 Å ^e Cholesterics: 2000 Å
L	Crossover length for logarithmic divergences	(2.31)	10^4 Å— 10^{23} km
Dimensionless parameters			
w_0	$k_B T/B'_0 \lambda_0^3 \equiv t_0 \lambda_0^{-3}$		Bilayers: 1 Monolayers: 5
κ	$K_1^0/\rho_0(\eta_3^0)^2$		10^{-4}
Miscellaneous			
a_1, a_2, a_4, a_5	Coefficients of $1/\omega$ divergences	(1.1)	B^{2f}
μ^2	Coefficient of logarithmic divergence of η_3	(4.22)	B^2

^aReference 7.

^bReference 8.

^cReference 9.

^dReferences 7 and 10.

^eReference 3.

^fLowest order in temperature results for these quantities are given in Eq. (4.25)

perature are given by (4.25).

The viscosity η_3 does not diverge as $1/\omega$ at low frequencies. It does, however, have a much weaker logarithmic divergence given by (4.36) below.

One operational consequence of these divergences is that the sound attenuations at low frequencies should be far (divergently) stronger in these systems than predicted by classical hydrodynamics. The first ($i=1$) and second ($i=2$) sound^{6,11,12} modes in these systems propagate with wave numbers

$$q_i = \omega/c_i(\theta) + i\alpha_i(\theta, \omega), \quad (1.4)$$

where θ is the angle between the direction of propagation and the z axis, the $c_i(\theta)$ are the direction-dependent speeds of sound, and the $\alpha_i(\theta, \omega)$ are the attenuations. In conventional hydrodynamics $\alpha_i(\theta, \omega)/\omega^2$ would approach a finite θ -dependent constant proportional to a linear combination of viscosities, at low frequencies. Our results imply that the attenuation obeys

$$\alpha_i/\omega^2 = f_i(\theta)/\omega + g_i(\theta) \quad (1.5)$$

which diverges as $1/\omega$ at low frequencies. The $g_i(\theta)$ term in (1.5) corresponds to the contributions of η_i^0 in (1.1). The coefficients of the $1/\omega$ term in (1.5), $f_i(\theta)$, are plotted as a function of θ in Fig. 3 and are given explicitly¹³ by (4.26).

Using the numerical estimates in Table I, we find that the anomalous part of the attenuation [proportional to $f_i(\theta)\omega$] starts¹⁴ to dominate over the "conventional background" [proportional to $g_i(\theta)\omega^2$] at frequencies around 10^6 – 10^8 Hz, which are in the range of ultrasound experiments. And indeed, ultrasonic experiments have long shown^{15–17} that $\alpha_i(\theta, \omega)$ does not scale like ω^2 as predicted

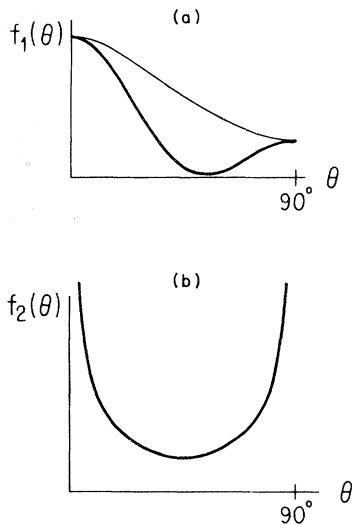


FIG. 3. Plots of the coefficient of the anomalous (linear in ω) part of the sound attenuation as a function of direction of propagation θ ($\theta=0$ is the z axis). (a) Shows $f_1(\theta)$ (first sound attenuation). Thick line is for $a_5 < 0$; the thin, $a_5 > 0$. (b) Shows $f_2(\theta)$ (second sound attenuation), which has the same qualitative behavior for either sign of a_5 .

by conventional hydrodynamics. A recent reanalysis of this data¹⁸ shows a good fit to our predictions as summarized by (1.5). In particular the anomalous part agrees quite well with (4.26) for reasonable values¹⁹ for the parameters a_i , and the conventional part of the attenuation $g_i(\theta)$ is virtually identical with the full attenuation in the nematic phase of the same material (where that phase exists), and fairly close²⁰ to that of the isotropic phase in those materials which lack a nematic phase.

A detailed test of (1.1) is not, strictly speaking, possible from attenuation measurements alone, since, as is evident from (4.26), only the sum $\eta_2 + \eta_4$ is determined by the fit. Fortunately, since η_2 is a shear viscosity, it can be determined independently of the bulk viscosities η_1 , η_4 , and η_5 (which only affect the damping of *compressional* modes) by, say, a mechanical shear impedance experiment.²¹

A more direct way of measuring η_2 is via a steady shear flow experiment. We discuss such an experiment in Sec. V and argue that the flow should be non-Newtonian in the sense that the effective viscosity should depend divergently on the shear rate. Non-Newtonian shear flow has been observed by Kim *et al.*²² and Bhattacharya and Letcher,²³ as discussed in Sec. V. A detailed calculation of this shear dependence is now in progress.²⁴

All of these striking effects are ultimately due to the rotation invariance of these systems, which renders the energy cost of the undulation mode (Fig. 2) very small at long wavelengths. An external magnetic field breaks the rotational invariance of the system and renders the zero-frequency and -wave-number components of the viscosities finite. These viscosities, given explicitly by (4.39), diverge at small field H as H^{-2} .

Divergences are not restricted to the four viscosities discussed so far. Grinstein and Pelcovits² have shown that the elastic constants B' and K_1 (see Table I), respectively, vanish and diverge logarithmically at long wavelengths. We have extended their calculation to the elastic constants A , B , and C . The latter two vanish as $(\ln q)^{-4/5}$ at small q , while the former shows an initial logarithmic dependence on q , but ultimately levels off at a finite value as $q \rightarrow 0$. Detailed expressions for these quantities are given by (2.24). We show in Sec. III that A , B , C , and K_1 depend *only* on wave vector, and not on frequency.

These "static" divergences could, in principle, be measured through sound *speed* experiments; they appear, however, to be much more difficult to detect than the spectacular effects on the attenuation.

In Sec. II we construct an elastic theory for the equilibrium behavior of these systems, extending the work of Grinstein and Pelcovits² to include a coupling to the density and the velocity field. This is then used in Sec. III as an input to the nonlinear fluctuating hydrodynamical theory we develop. We discuss how to extract effective viscosities in the presence of nonlinearities and fluctuations with the use of perturbation theory in temperature. In Sec. IV we implement this theory and derive expressions for all the divergent viscosities as functions of \vec{q} , ω , and H . In Sec. V we discuss the non-Newtonian shear flow predicted by our theory, summarize the existing experimental evidence for our predictions, and suggest further experiments.

II. BREAKDOWN OF CONVENTIONAL ELASTIC THEORY

A. Construction of the effective Hamiltonian

In formulating a hydrodynamic theory of any system it is necessary to consider only those "slow" variables whose relaxation times diverge as the length scale of their fluctuations goes to infinity. Such "hydrodynamic relaxation" occurs^{25,26} when the variable in question is the local density of a conserved quantity or when there is no restoring force in response to an "infinite-wavelength disturbance" of the variable from its equilibrium value. In the former case, the infinite-wavelength mode *is* the conserved quantity, and hence cannot relax. The latter includes order-parameter fluctuations near a continuous phase transition as well as the Nambu-Goldstone modes associated with a spontaneously broken continuous symmetry. In smectics-*A*, the symmetry that is broken is translational invariance,^{3,27} due to the spontaneous layering (see Fig. 1). The hydrodynamic variable associated with this is the displacement $u(\vec{x})$ of the layers in the direction normal to themselves²⁸ (see Fig. 2). The other hydrodynamic variables in smectics-*A* are just the conserved mass and momentum densities $\rho(\vec{x})$ and $\vec{g}(\vec{x})$, respectively.

Our next step in discussing either the static or the dynamic behavior of these materials is to construct a phenomenological effective Hamiltonian for these variables that is consistent with the translational and rotational invariance of the system. Translational invariance requires that the Hamiltonian involve only gradients of u , while rotational invariance implies that these gradients can only enter in combinations which vanish when evaluated for configurations $u(\vec{x})$ that correspond to pure rotations. The invariants that satisfy these constraints and involve only linear and quadratic terms in u are³ $\nabla^2 u$ and

$$E(u) = \nabla_z u - \frac{1}{2}(\vec{\nabla} u)^2. \quad (2.1)$$

The most general effective Hamiltonian^{3,6,12} one can construct, to quadratic order in these invariants and lowest order in $\delta\rho = \rho - \rho_0$ and \vec{g} is

$$F[u, \rho, \vec{g}] = \frac{1}{2} \int d^3x \left[BE^2(u) + K_1(\nabla^2 u)^2 + \Delta E(u) + A \left[\frac{\delta\rho}{\rho_0} \right]^2 + CE(u) \frac{\delta\rho}{\rho_0} + \frac{(\vec{g})^2}{\rho} + 3k_B T \ln \left[\frac{\rho}{\rho_0} \right] \right], \quad (2.2)$$

where the penultimate term is just the kinetic energy, and the ultimate term insures that ρ_0 is the quiescent (equilibrium) density. Higher-order terms in this expansion can be shown to be irrelevant to the long-wavelength behavior of the system. Stability requires that the elastic moduli A , B , C , and K_1 satisfy $A, K_1 > 0$ and $B > C^2/A$.

In considering the static (equal-time) correlations of u and ρ , we can first integrate the momentum density \vec{g} out of the probability distribution to obtain an effective Hamiltonian for ρ and u alone:

$$F[u, \rho] = -\beta^{-1} \ln \left[\int \mathcal{D}(\vec{g}) e^{-\beta F(u, \rho, \vec{g})} \right] = \frac{1}{2} \int d^3x \left[BE^2(u) + K_1(\nabla^2 u)^2 + \Delta E(u) + A \left[\frac{\delta\rho}{\rho_0} \right]^2 + CE(u) \frac{\delta\rho}{\rho_0} \right], \quad (2.3)$$

where $\beta^{-1} = k_B T$. Note that the result of integrating out \vec{g} has simply been to cancel the last two terms of (2.2). If we repeat this technique and integrate $\delta\rho$ out of the probability distribution as well, we obtain the effective Hamiltonian of Grinstein and Pelcovits² with their parameters t , λ , and B (called B' here) related to the elastic constants defined here as given in Table I.

We shall be interested in calculating the various equal-time correlation functions

$$\chi_{\alpha\beta}(\vec{x} - \vec{x}') = \langle \delta\psi_\alpha(\vec{x}) \delta\psi_\beta(\vec{x}') \rangle, \quad (2.4)$$

where the brackets indicate the equilibrium average

$$\langle A \rangle = \int \mathcal{D}(\rho) \mathcal{D}(\vec{g}) \mathcal{D}(u) P[u, \rho, \vec{g}] A \quad (2.5a)$$

and the equilibrium probability distribution $P[u, \rho, \vec{g}]$ is given by

$$P[u, \rho, \vec{g}] = e^{-\beta F[u, \rho, \vec{g}]} / Z, \quad (2.5b)$$

Z being the partition function. The labels α and β in (2.4) run over the set ρ , u , and \vec{g} such that, for example, $\psi_\rho(\vec{x}) \equiv \rho(\vec{x})$. In (2.4), $\delta\psi_\alpha(\vec{x}) = \psi_\alpha(\vec{x}) - \langle \psi_\alpha(\vec{x}) \rangle$. We shall also be interested in the inverse correlation functions $(\chi^{-1})_{\alpha\beta}$ defined by

$$[\chi^{-1}(\vec{q})]_{\alpha\gamma} \chi_{\gamma\beta}(\vec{q}) = \delta_{\alpha\beta}, \quad (2.6)$$

where a sum over the repeated index γ is implied and $\chi_{\alpha\beta}(\vec{q})$ is the Fourier transform of $\chi_{\alpha\beta}(\vec{x} - \vec{x}')$.

In finalizing our definition of our model we must, as discussed in Ref. 2, choose the parameter Δ in (2.2) such that $\langle \nabla_z u \rangle = 0$ if the state we describe as $u = 0$ is to be a true minimum²⁹ of the free energy.

B. Renormalization-group treatment

We shall now treat the Hamiltonian (2.3) using the momentum shell renormalization group (RG). We start by confining the wave vectors of the Fourier-transformed variables $\rho(\vec{q})$ and $u(\vec{q})$ to a cylindrical Brillouin zone (i.e., $|\vec{q}_\perp| < \Lambda$ and $-\infty < q_z < \infty$). The parameter Λ should be comparable in magnitude to the inverse of the layer spacing a . We then proceed to integrate the degrees of freedom at the shortest length scales out of the probability distribution. Specifically, we integrate those components of the field in the infinitesimal shell $b^{-1} < \vec{q}_\perp/\Lambda < 1$ where $b = 1 + \delta l$. After anisotropically rescaling wave vectors³⁰ ($\vec{q}_\perp \rightarrow \vec{q}_\perp b$ and $q_z \rightarrow q_z b^2$) and fields

$$u(\vec{q}_\perp, q_z) = Z_u u(b \vec{q}_\perp, b^2 q_z), \quad (2.7a)$$

$$\rho(\vec{q}_\perp, q_z) = Z_\rho \rho(b \vec{q}_\perp, b^2 q_z) \quad (2.7b)$$

one is returned to a Hamiltonian of the form (2.3) (plus "irrelevant" terms) but with changed (or "renormalized")

parameters A , B , C , and K_1 . The integration over short-wavelength degrees of freedom is done perturbatively in the anharmonicities, the small dimensionless parameter being $w = t\lambda^{-3}$. Since such an analysis is now rather standard, and because of the detailed discussion in Ref. 2, we will not go into the graphical implementation of this perturbative calculation. It is crucial, however, for our later dynamical calculation, that only the u - u propagator is important and the dominant fluctuations are those with wave vectors $q_z \sim \lambda q^2$.

By calculating the renormalization of the $(\nabla_z u)^2$ term in the Hamiltonian at one-loop order we find the following recursion relation for the renormalized elastic modulus B :

$$B_R = \frac{Z_u^2}{b^8} \left[B - \frac{wt}{16\pi} \beta B^2 \delta l \right] + O(w^2). \quad (2.8)$$

By calculating the renormalization of the coefficients of $(\nabla_z u)(\vec{\nabla} u)^2$, and $|\vec{\nabla} u|^4$, we also obtain the relations for B_R :

$$B_R = \frac{Z_u^3}{b^{12}} \left[B - \frac{wt}{16\pi} \beta B^2 \delta l \right] + O(w^2) \quad (2.9)$$

and

$$B_R = \frac{Z_u^4}{b^{16}} \left[B - \frac{wt}{16\pi} \beta B^2 \delta l \right] + O(w^2) \quad (2.10)$$

which will be consistent with each other and with (2.8) only if we choose

$$Z_u = b^4 \quad (2.11)$$

which implies

$$B_R = B - \frac{wt}{16\pi} \beta B^2 \delta l + O(w^2). \quad (2.12)$$

Similar arguments for the coefficients of $\delta\rho \nabla_z u$ and $(\delta\rho)(\vec{\nabla} u)^2$ give the renormalized elastic modulus

$$C_R = C - \frac{wt}{16\pi} \beta B C \delta l + O(w^2) \quad (2.13)$$

and

$$Z_\rho = b^2. \quad (2.14)$$

With the rescalings Z_u and Z_ρ now determined, we can readily show that the renormalized A and K_1 obey the following:

$$A_R = A - \frac{wt}{16\pi} \beta C^2 \delta l + O(w^2), \quad (2.15)$$

$$K_{1R} = K_1 + \frac{wK_1}{32\pi} \delta l + O(w^2). \quad (2.16)$$

We can rewrite these equations as differential equations satisfied by l -dependent elastic moduli

$$\frac{dA}{dl} = -\frac{wt}{16\pi} \beta C^2, \quad (2.17)$$

$$\frac{dB}{dl} = -\frac{wt}{16\pi} \beta B^2, \quad (2.18)$$

$$\frac{dC}{dl} = -\frac{wt}{16\pi} \beta B C, \quad (2.19)$$

$$\frac{dK_1}{dl} = \frac{w}{32\pi} K_1. \quad (2.20)$$

These equations can be used to form the recursion relations for t and w :

$$\frac{dt}{dl} = \frac{wt}{16\pi}, \quad (2.21)$$

$$\frac{dw}{dl} = \frac{-5w^2}{64\pi}, \quad (2.22)$$

which are precisely those found in Ref. 2 by starting with a Hamiltonian for u alone. Using this RG we can show that

$$\begin{aligned} \chi_{\alpha\beta}(\vec{q}_\perp, q_z, A, B, C, K_1) \\ = \exp(\lambda_{\alpha\beta} l) \chi_{\alpha\beta}(e^{l\vec{q}_\perp}, e^{2l} q_z, A(l), B(l), C(l), K_1(l)), \end{aligned} \quad (2.23)$$

where $\lambda_{pp}=0$, $\lambda_{pu}=\lambda_{up}=2$, and $\lambda_{uu}=4$. The utility of this relation becomes apparent when we analyze the solution of (2.22) for the coupling strength. We easily obtain

$$w(l) = \frac{w(0)}{1 + 5w(0)l/64\pi} \quad (2.24)$$

and observe that under repeated renormalization $l \rightarrow \infty$ and $w(l) \rightarrow 0$. This means that for large enough l we can evaluate the right-hand side of (2.23) in the harmonic approximation. Large enough, in this context, means that the modes of wave vector longer than that on the right-hand side have very small fluctuations; operationally, we shall impose this condition by choosing l such that the u - u propagator in the harmonic approximation,

$$\chi_{uu}^0 = t/(q_z^2 + \lambda^2 q^4), \quad (2.25)$$

evaluated at this wave vector, is smaller than its smallest value on the Brillouin-zone boundary. This leads to the choice

$$l = \ln\{\Lambda \max[q_\perp^{-1}, (\lambda/q_z)^{1/2}]\}. \quad (2.26)$$

Putting these results together we find, using (2.23), that the associated inverse correlation functions [see (2.6)] can be written as

$$[\chi^{-1}(\vec{q})]_{uu} = \beta[B_R(\vec{q})q_z^2 + K_{1R}(\vec{q})q^4], \quad (2.27)$$

$$[\chi^{-1}(\vec{q})]_{pu} = i\beta C_R(\vec{q})q_z, \quad (2.28)$$

$$[\chi^{-1}(\vec{q})]_{pp} = \beta A_R(\vec{q})/\rho_0, \quad (2.29)$$

where $A_R(q)$, $B_R(q)$, $C_R(q)$, and $K_{1R}(q)$ are just the $A(l)$, $B(l)$, $C(l)$, and $K_1(l)$ obtained from (2.16)–(2.19) and evaluated at the l given by (2.26). We easily obtain that

$$A_R(\vec{q}) = \frac{Az^{4/5}}{1 + t\beta B(z^{4/5} - 1)}, \quad (2.30a)$$

$$B_R(\vec{q}) = \frac{B}{1 + t\beta B(z^{4/5} - 1)}, \quad (2.30b)$$

$$C_R(\vec{q}) = \frac{C}{1 + t\beta B(z^{4/5} - 1)}, \quad (2.30c)$$

$$K_{1R}(\vec{q}) = K_1 z^{2/5} \quad (2.30d)$$

with $z = 1 + 5wl/64\pi$ and l given by (2.26). These results imply those of Ref. 2 for t and λ . Note that $B_R(q)$ and $C_R(q)$ vanish logarithmically at small wave vector as $|\ln q|^{-4/5}$ while $A_R(q)$ after an initial logarithmic correction approaches a constant.

This asymptotic behavior will only appear on length scales

$$L > a \exp(64\pi/5w) \quad (2.31)$$

which may be quite large ($> 10^{23}$ m) for typical values of w (~ 0.7). The additive logarithmic dependence obtained upon expanding (2.30) for small l should, however, be observable.

C. Extension to hexatics-B

Due to the breaking of rotational symmetry in the planes of the smectic layers, hexatics have an angle ϕ as a new hydrodynamic variable. The Hamiltonian which includes gradients of ϕ up to quadratic order and is consistent with all the symmetries is

$$F = F_A + \frac{1}{2} \int d^3x [K_\perp (\vec{\nabla}_\perp \phi)^2 + K_z (\nabla_z \phi)^2 + (J_\perp \nabla_\perp^2 \phi + J_z \nabla_z^2 \phi) E(u)], \quad (2.32)$$

where F_A is the Hamiltonian (2.2) of the smectic A . Note the absence of terms like $\nabla_z u \nabla_z \phi$ and $\vec{\nabla}_\perp u \cdot \vec{\nabla}_\perp \phi$, both of which are forbidden by inversion symmetry ($u \rightarrow -u, z \rightarrow -z$). It is a simple exercise in power counting to show that the terms proportional to J_\perp and J_z which couple u and ϕ are irrelevant. Hence the additional variable ϕ has no effect on the fluctuations of u at long length scales, and the results derived above apply in their entirety to hexatics-B, as well as smectics-A.

III. FLUCTUATING NONLINEAR HYDRODYNAMICS FOR SMECTICS-A

A. Langevin equations

In deriving a fluctuating nonlinear hydrodynamic description of smectic-A liquid crystals we follow the formal development of Ma and Mazenko.³¹ In this approach the dynamics of the hydrodynamic variables³² introduced in Sec. II are governed by a Langevin equation

$$\frac{\partial \psi_i(t)}{\partial t} = V_i[\psi(t)] - L_{ij} \frac{\partial F}{\partial \psi_j(t)} + f_i. \quad (3.1)$$

The reversible part of the dynamics is contained in the "streaming term"

$$V_i[\psi] = Q_{ij}(\psi) \frac{\partial F}{\partial \psi_j(t)} - \beta^{-1} \frac{\partial}{\partial \psi_j(t)} Q_{ij}(\psi), \quad (3.2)$$

where $Q_{ij}(\psi) = \{\psi_i, \psi_j\}$ is the Poisson bracket between the variables ψ_i , and $F(\psi)$ is the effective Hamiltonian given in this case by (2.2). The damping coefficients L_{ij} and the thermal noise f_i characterize the irreversible, dissipative part of the dynamics. The noise is assumed to be normally distributed with zero mean and obeys the fluctuation-dissipation relation

$$\langle f_i(t) f_j(t') \rangle = 2k_B T L_{ij} \delta(t - t'). \quad (3.3)$$

In deriving Poisson bracket relations we use the microscopic definitions for the fields

$$\rho(\vec{x}) = \sum_\alpha m \delta(\vec{x} - \vec{r}_\alpha), \quad (3.4)$$

$$\rho(x) u(\vec{x}) = \sum_\alpha u_\alpha \delta(\vec{x} - \vec{r}_\alpha), \quad (3.5)$$

$$\vec{g}(\vec{x}) = \sum_\alpha \vec{p}_\alpha \delta(\vec{x} - \vec{r}_\alpha), \quad (3.6)$$

where \vec{r}_α is the center-of-mass coordinate of the α th molecule in the liquid crystal, \vec{p}_α is its momentum, m its mass, and u_α the z component of its displacement from the mean position imposed by the one-dimensional ordering. The canonical Poisson brackets

$$\{u_\alpha, p_\beta^i\} = \delta_{i\alpha} \delta_{\alpha\beta}, \quad (3.7)$$

$$\{r_\alpha^j, p_\beta^i\} = \delta_{ij} \delta_{\alpha\beta} \quad (3.8)$$

lead to the relations

$$\{\rho(x), g^i(x')\} = -\nabla_x^i [\delta(\vec{x} - \vec{x}') \rho(\vec{x})], \quad (3.9)$$

$$\{u(x), g^i(\vec{x}')\} = \delta(\vec{x} - \vec{x}') [\delta_{iz} - \nabla_x^i u(\vec{x})], \quad (3.10)$$

$$\{g_i(\vec{x}), g_j(\vec{x}')\} = -\nabla_x^j [\delta(\vec{x} - \vec{x}') g^i(\vec{x})] + \nabla_x^i [\delta(\vec{x} - \vec{x}') g^j(\vec{x})] \quad (3.11)$$

between the macroscopic variables. The dissipative coefficients are chosen to agree with those in the linearized theory.⁶ Thus, since the equation of motion for ρ must reduce to the continuity equation, we have $L_{\rho\rho} = 0$. In the equation of motion for u there is a time-dependent-Ginzburg-Landau type of dissipation⁶ with $L_{uu} = \Gamma$. Finally, there is the dissipation for the momentum density due to viscous drag, which can be expressed in terms of the viscous part of the stress tensor, σ_{ij}^D , via³³

$$L_{ij}^D g_j = \nabla_j \sigma_{ij}^D \quad (3.12)$$

with

$$\sigma_{ij}^D = -\eta_{ijkl} \nabla_l \frac{\delta F}{\delta g_k}, \quad (3.13)$$

where the viscosity tensor η_{ijkl} has the general form for a uniaxial system

$$\eta_{ijkl} = \eta_2 (\delta_{il} \delta_{jk} + \delta_{ij} \delta_{kl}) + (\eta_3 - \eta_2) [\delta_{iz} (\delta_{jl} \delta_{kz} + \delta_{lj} \delta_{kz}) + \delta_{iz} (\delta_{jk} \delta_{lz} + \delta_{kz} \delta_{lj})] + (\eta_4 - \eta_2) \delta_{ij} \delta_{kl} + (\eta_1 + \eta_2 - 4\eta_3 + \eta_4 - 2\eta_5) \delta_{iz} \delta_{jz} \delta_{kz} \delta_{lz} + (\eta_5 - \eta_4 + \eta_2) (\delta_{ij} \delta_{kz} \delta_{lz} + \delta_{kl} \delta_{iz} \delta_{jz}). \quad (3.14)$$

It is then a straightforward matter to identify the Fourier transform of the damping for the momentum density \vec{g} as

$$L_{ij}^g(\vec{q}) = \eta_4 q_i q_j + \delta_{ij} \Gamma_1(\vec{q}) + \delta_{iz} \delta_{jz} \Gamma_2(\vec{q}) + q_z (q_i \delta_{jz} + q_j \delta_{iz}) \Gamma_3, \quad (3.15)$$

where

$$\Gamma_1(\vec{q}) = \eta_2 q_1^2 + \eta_3 q_z^2, \quad (3.16a)$$

$$\Gamma_2(\vec{q}) = (\eta_3 - \eta_2) q^2 + (\eta_1 + \eta_2 - 4\eta_3 + \eta_4 - 2\eta_5) q_z^2, \quad (3.16b)$$

$$\Gamma_3 = \eta_5 + \eta_3 - \eta_4. \quad (3.16c)$$

The associated noise terms are given by $f_\rho = 0$, $f_u = \theta$, and $f_g^i = \zeta_i$ and, from (3.3), satisfy

$$\langle \theta(\vec{x}, t) \theta(\vec{x}', t') \rangle = 2k_B T \Gamma \delta(\vec{x} - \vec{x}') \delta(t - t'), \quad (3.17)$$

$$\langle \theta(\vec{x}, t) \zeta_i(\vec{x}', t') \rangle = 0, \quad (3.18)$$

$$\begin{aligned} \langle \zeta_i(\vec{x}, t) \zeta_j(\vec{x}', t') \rangle &= 2\rho_0 k_B T \eta_{ijkl} \nabla_k \nabla_l' \delta(\vec{x} - \vec{x}') \delta(t - t') \\ &= 2\rho_0 k_B T L_{ij}^g(\vec{x}) \delta(\vec{x} - \vec{x}') \delta(t - t'). \end{aligned} \quad (3.19)$$

The nonlinear equations of motion are now completely defined, but there are a few rearrangements which put them in a more familiar form. The streaming velocity associated with the various fields can be written as

$$V_\rho = -\vec{\nabla} \cdot \left[\rho \frac{\delta F}{\delta \vec{g}} \right], \quad (3.20)$$

$$V_u = \frac{\partial E}{\partial (\nabla_i u)} \frac{\delta F}{\delta g_i}, \quad (3.21)$$

$$\begin{aligned} V_g^i &= \rho \nabla_i \left[\frac{\delta F}{\delta \rho} \right] - \frac{\partial E}{\partial (\nabla_i u)} \frac{\partial F}{\partial u} \\ &\quad - g_j \nabla_i \left[\frac{\delta F}{\delta g_j} \right] - \nabla_j \left[g_i \frac{\delta F}{\delta g_j} \right]. \end{aligned} \quad (3.22)$$

It is not difficult to show³⁴ that V_g^i can be written in terms of the divergence of the reactive part of the stress tensor:

$$V_g^i = \nabla_j \sigma_{ij}^R, \quad (3.23)$$

where σ_{ij}^R is symmetric and given by

$$\begin{aligned} \sigma_{ij}^R &= \frac{g_i g_j}{\rho} + \delta_{ij} \left[CE + \frac{A(\delta \rho)^2}{2\rho_0^2} - \frac{BE^2}{2} - \Delta E - \frac{1}{2} K \sum_{k,l} (\nabla_k \nabla_l u)^2 \right] + \left[C \frac{\delta \rho}{\rho_0} + BE + \Delta \right] \frac{\partial E}{\partial (\nabla_i u)} \frac{\partial E}{\partial (\nabla_j u)} \\ &\quad + K_1 \left[\frac{\partial E}{\partial (\nabla_j u)} \nabla^2 \nabla_i u + \frac{\partial E}{\partial (\nabla_i u)} \nabla^2 \nabla_j u \right] - K_1 \nabla_k \left[\frac{\partial E}{\partial (\nabla_k u)} \right] \nabla_i \nabla_j u. \end{aligned} \quad (3.24)$$

The symmetry $\sigma_{ij} = \sigma_{ij}^R + \sigma_{ij}^D = \sigma_{ji}$ guarantees that the angular momentum is conserved, i.e., that

$$\frac{\partial}{\partial t} L_i = -\nabla_k M_{ik}, \quad (3.25)$$

where

$$L_i = \epsilon_{ijk} x_j g_k \quad (3.26)$$

is the angular momentum density and

$$M_{ik} = \epsilon_{ijl} x_j \sigma_{lk} \quad (3.27)$$

is the angular momentum current. Summarizing these results, we have the equations of motion^{35,36}

$$\frac{\partial \rho}{\partial t} + \vec{\nabla} \cdot \vec{g} = 0, \quad (3.28)$$

$$\frac{\partial u}{\partial t} + \frac{\vec{g}}{\rho} \cdot \vec{\nabla} u = \frac{g_z}{\rho} - \Gamma \frac{\delta F}{\delta u} + \theta, \quad (3.29)$$

$$\frac{\partial g_i}{\partial t} = -\nabla_j \sigma_{ij} + \zeta_i. \quad (3.30)$$

B. Fokker-Planck description

In the rest of the paper we will be interested primarily in extracting the transport properties (speeds of sound, observable viscosities, and sound attenuation) from the equa-

tions of motion given above. These properties, in the case of a strongly nonlinear system, are conveniently defined in terms of the location and widths of the poles associated with the time and space Fourier transform of the time correlation function

$$C_{ij}(t) = \langle \delta \psi_j \delta \psi_i(t) \rangle. \quad (3.31)$$

Thus we must develop methods for calculating $C_{ij}(t)$. In carrying out this development it is convenient to go from a Langevin-equation description to a Fokker-Planck description. The connection between these two descriptions is discussed in Ref. 31 where it is shown that $C_{ij}(t)$ can be written in the form

$$C_{ij}(t) = \langle \delta \psi_j e^{\tilde{D}_\psi t} \delta \psi_i \rangle, \quad (3.32)$$

where the average is defined by (2.5) and the time evolution of the fields is governed by the generalized Fokker-Planck operator

$$\tilde{D}_\psi = \left[V_i(\psi) \delta_{ij} - L_{ij} \left[-\beta^{-1} \frac{\partial}{\partial \psi_i} + \frac{\partial F}{\partial \psi_i} \right] \right] \frac{\partial}{\partial \psi_j}. \quad (3.33)$$

Note that \tilde{D}_ψ is specified by the same quantities that entered the Langevin equation. It will be useful to introduce the adjoint operator

$$\tilde{D}_\psi^\dagger = \left[-V_i(\psi)\delta_{ij} - L_{ij} \left[-\beta^{-1} \frac{\partial}{\partial \psi_i} + \frac{\partial F}{\partial \psi_i} \right] \right] \frac{\partial}{\partial \psi_j} \quad (3.34)$$

which satisfies

$$\langle A(\psi) \tilde{D}_\psi B(\psi) \rangle = \langle B(\psi) \tilde{D}_\psi^\dagger A(\psi) \rangle. \quad (3.35)$$

The proof of (3.35) is facilitated by the use of the theorem stating that the reversible Hamiltonian dynamics generated by the streaming term V_i leads to a divergenceless probability current in phase space:

$$\frac{\partial}{\partial \psi_i} [V_i(\psi) P(\psi)] = 0, \quad (3.36)$$

where $P(\psi)$ is the equilibrium probability distribution given, in this case, by (2.5b).

The simplest approach³⁷ to the calculation of these correlation functions is to calculate their Laplace transform

$$C_{ij}(z) = -i \int_0^\infty dt e^{izt} C_{ij}(t) \quad (3.37)$$

which, with the use of (3.32), can be rewritten as

$$C_{ij}(z) = \langle \delta \psi_j R(z) \delta \psi_i \rangle, \quad (3.38)$$

where

$$R(z) = (z - i\tilde{D}_\psi)^{-1} \quad (3.39)$$

is the resolvent operator. Nonlinear contributions to the dynamical behavior can be treated most directly through the memory function $M_{ij}(z)$ defined by

$$M_{ik} \langle (i\tilde{D}_\psi^\dagger \delta \psi_j) R(z) \delta \psi_k \rangle = \langle \delta \psi_l R(z) (i\tilde{D}_\psi \delta \psi_l) \rangle [\underline{C}^{-1}(z)]_{lk} \langle (i\tilde{D}_\psi^\dagger \delta \psi_j) R(z) \delta \psi_k \rangle. \quad (3.47)$$

Taking this term to the other side of (3.46), we see that the memory function $M_{ij}(z)$ can be written as the sum of two pieces

$$M_{ij}(z) = M_{ij}^{(s)} + M_{ij}^{(c)}(z). \quad (3.48)$$

The static contribution is given by

$$M_{ij}^{(s)} = K_{ik}^{(s)} (\underline{\chi}^{-1})_{kj}, \quad (3.49)$$

where

$$K_{ij}^{(s)} = \langle \delta \psi_j i\tilde{D}_\psi \delta \psi_i \rangle \quad (3.50)$$

and the dynamic (frequency-dependent) contribution is given by

$$M_{ij}^{(c)}(z) = K_{ik}^{(c)}(z) (\underline{\chi}^{-1})_{kj} \quad (3.51)$$

with

$$K_{ij}^{(c)}(z) = -\langle I_j^\dagger R(z) I_i \rangle + \langle \delta \psi_l R(z) I_i \rangle [\underline{C}^{-1}(z)]_{lk} \langle I_j^\dagger R(z) \delta \psi_k \rangle, \quad (3.52)$$

where we have introduced the notation

$$[z\delta_{ik} - M_{ik}(z)] C_{kj}(z) = \chi_{ij}, \quad (3.40)$$

where

$$\chi_{ij} = C_{ij}(t=0) = \langle \delta \psi_j \delta \psi_i \rangle. \quad (3.41)$$

The poles of the spatial Fourier transform of $C_{ij}(z)$ are associated with the zeros of the matrix $z\underline{1} - \underline{M}(z)$. Clearly $\underline{M}(z)$ carries direct information about the position (sound speeds) and widths (damping) of the hydrodynamical modes in the system. For future reference we also define the "propagator" $G_{ij}(z)$ via

$$[z\delta_{ik} - M_{ik}(z)] G_{kj}(z) = \delta_{ij}. \quad (3.42)$$

We can derive convenient expressions for $M_{ik}(z)$ by using the operator identity

$$zR(z) = 1 + R(z) i\tilde{D}_\psi \quad (3.43a)$$

$$= 1 + i\tilde{D}_\psi R(z) \quad (3.43b)$$

in (3.38) to obtain

$$zC_{ij}(z) = \chi_{ij} + \langle \delta \psi_j R(z) i\tilde{D}_\psi \delta \psi_i \rangle. \quad (3.44)$$

Comparing this equation with (3.40) we identify

$$M_{ik}(z) C_{kj}(z) = \langle \delta \psi_j R(z) i\tilde{D}_\psi \delta \psi_i \rangle. \quad (3.45)$$

Multiplying this equation by z and using the identity (3.43b) on each side leads to the result

$$M_{ik} [\chi_{kj} + \langle (i\tilde{D}_\psi^\dagger \delta \psi_j) R(z) \delta \psi_k \rangle] = \langle \delta \psi_j i\tilde{D}_\psi \delta \psi_i \rangle + \langle (i\tilde{D}_\psi \delta \psi_j) R(z) (i\tilde{D}_\psi^\dagger \delta \psi_i) \rangle. \quad (3.46)$$

If we use (3.45) we can rewrite the second term on the left in (3.46) as

$$(\underline{\chi}^{-1})_{ik} \chi_{kj} = \delta_{ij}, \quad (3.53)$$

$$C_{ik}(z) [\underline{C}^{-1}(z)]_{kj} \equiv \delta_{ij}, \quad (3.54)$$

and

$$I_i(\psi) = \tilde{D}_\psi \delta \psi_i = V_i - L_{ik} \frac{\partial F}{\partial \psi_k}, \quad (3.55)$$

$$I_j^\dagger(\psi) = \tilde{D}_\psi^\dagger \delta \psi_j = -V_j - L_{jk} \frac{\partial F}{\partial \psi_k}. \quad (3.56)$$

C. Quasilinear approximation

We consider here the approximation where we neglect the dynamic part of the memory function. As we shall see later, this approximation involves ignoring the dynamic nonlinear contributions. It does include static nonlinear contributions through the exact static correlation functions χ_{ij} which enter the static memory function $M^{(s)}$ as seen in (3.49).

We can evaluate the quantity $K_{ij}^{(s)}$, defined by (3.50), by

using (3.55) and carrying out a functional integration by parts to obtain the simple result

$$K_{ij}^{(s)} = i\beta^{-1} \langle Q_{ij} \rangle - i\beta^{-1} L_{ij} . \quad (3.57)$$

It is straightforward to evaluate the averages of the various Poisson brackets given by (3.9)–(3.11) and determine $K_{ij}^{(s)}$. Combining this result with (3.49) and (3.40) we obtain the equations of motion for the correlation functions:

$$zC_{\rho\alpha}(z) - q_i C_{g_i\alpha}(z) = \chi_{\rho\alpha} , \quad (3.58a)$$

$$zC_{u\alpha}(z) - i\rho_0^{-1} C_{g_z\alpha}(z) + i\beta^{-1} \Gamma(\chi^{-1})_{uu} C_{u\alpha}(z) = \chi_{u\alpha} , \quad (3.58b)$$

$$zC_{g_i\alpha}(z) + \beta^{-1} [-q_i(\chi^{-1})_{\rho\rho}\rho_0 + i\delta_{iz}(\chi^{-1})_{\rho u}] C_{\rho\alpha}(z) + \beta^{-1} [-q_i\rho_0(\chi^{-1})_{\rho u} + i\delta_{iz}(\chi^{-1})_{uu}] C_{u\alpha}(z) + i\rho_0^{-1} L_{ik} C_{g_k\alpha}(z) = \chi_{g_i\alpha} , \quad (3.58c)$$

where the index α runs over values ρ , u , and \vec{g} . We can then solve these equations in the small- \vec{q} and $-z$ limit to obtain the hydrodynamic pole structure. This just involves solving for the zeros of the determinant of $(z\mathbb{I} - \underline{M}^{(s)})$. There are two pairs of solutions of the form given by (1.4) where the sound speeds⁶ are related to the renormalized elastic moduli defined by (2.27), (2.28), and (2.29) by

$$\rho_0(c_1^2 + c_2^2) = A_R + (B_R - 2C_R)\cos^2\theta , \quad (3.59a)$$

$$\rho_0^2 c_1^2 c_2^2 = (A_R B_R - C_R^2)\sin^2\theta \cos^2\theta . \quad (3.59b)$$

The sound attenuation is given by

$$\begin{aligned} \frac{\alpha_i(\theta)}{\omega^2} &= \frac{(-1)^i}{2\rho_0 c_1^3(\theta)[c_1^2(\theta) - c_2^2(\theta)]} \{ \sin^2\theta \cos^2\theta [\eta_1 A_R + (\eta_2 + \eta_4)(A_R + B_R - 2C_R) + 2\eta_3(C_R - 2A_R) + 2\eta_5(C_R - A_R)] \\ &\quad + \eta_3[A_R + (B_R - 2C_R)\cos^4\theta] + \Gamma B_R(C_R \cos^2\theta + A_R)\cos^2\theta \\ &\quad - \rho_0 c_i^2(\theta)[(\eta_1 + \Gamma B_R)\cos^2\theta + (\eta_2 + \eta_4)\sin^2\theta + \eta_3] \} . \end{aligned} \quad (3.60)$$

In Sec. IV we shall carry out a perturbative analysis of the nonlinear corrections to the transport coefficients which will require the evaluation of integrals of products of correlation functions over wave number and frequency. Fortunately, since the dominant contribution to these integrals comes from the region (see Sec. II) $\omega \sim q_z \sim \lambda q^2$, we only need detailed expressions for the correlation functions that contribute to the integrals in this regime. As we now show, the resulting expressions for the correlation functions are relatively simple.

As a first step in developing this analysis let us introduce an ordering parameter ϵ such that $q_\perp \sim O(\epsilon)$, $q_z \sim O(\epsilon^2)$, and $z \sim O(\epsilon^2)$. We can then, using (2.27), (2.28), and (2.29), make the estimates

$$(\chi^{-1})_{uu} \sim O(\epsilon^{-4}) , \quad (3.61a)$$

$$(\chi^{-1})_{u\rho} \sim O(\epsilon^{-2}) , \quad (3.61b)$$

$$(\chi^{-1})_{\rho\rho} \sim O(1) . \quad (3.61c)$$

Since we will need an explicit expression for $C_{uu}(\vec{q}, z)$, we will concentrate on (3.58) with $\alpha = u$. Ignoring higher-order terms in ϵ , these equations reduce to

$$zC_{\rho u} - q_i C_{g_i u} = \chi_{\rho u} , \quad (3.62a)$$

$$zC_{uu} - i\rho_0^{-1} C_{g_z u} = \chi_{uu} , \quad (3.62b)$$

$$(z + i\nu_3)q_i C_{g_i u} - A_R q^2 C_{\rho u} - i\rho_0 C_R q_z q^2 C_{uu} + i\nu_4 C_{g_z u} = 0 , \quad (3.62c)$$

$$\begin{aligned} (z + i\nu_2)C_{g_z u} - q_z(A_R - C_R)C_{\rho u} \\ - \rho_0[iC_R q_z^2 - i(\chi^{-1})_{uu}\rho_0^{-1}]C_{uu} + i\nu_1 q_i C_{g_i u} = 0 , \end{aligned} \quad (3.62d)$$

where

$$\nu_1 = q(\cos\theta)(\eta_3 + \eta_5) , \quad (3.63a)$$

$$\nu_2 = q^2[\eta_3 + \cos^2\theta(\eta_1 - 2\eta_3 - \eta_5)] , \quad (3.63b)$$

$$\nu_3 = q^2[\eta_2 + \eta_4 + \cos^2\theta(2\eta_3 + \eta_5 - \eta_2 - \eta_4)] , \quad (3.63c)$$

$$\begin{aligned} \nu_4 = q^3[\cos\theta(2\eta_3 + \eta_5 - \eta_2 - \eta_4) \\ + \cos^3\theta(\eta_1 + \eta_2 - 4\eta_3 - 2\eta_5 - \eta_4)] . \end{aligned} \quad (3.63d)$$

We easily find from these that ν_1 , ν_2 , and ν_3 are of $O(\epsilon^2)$, while ν_4 is of $O(\epsilon^4)$. Inserting the appropriate estimates for z , $\chi_{\rho u}$, and χ_{uu} in (3.62) leads to the estimates for $q_i C_{g_i u}$, $C_{\rho u}$, and C_{uu} shown in Table III. Using these estimates we can drop the $q_i C_{g_i u}$ and $C_{g_z u}$ terms in (3.62c) to obtain

$$C_{\rho u} = -iq_z \rho_0 (C_R / A_R) C_{uu} , \quad (3.64)$$

which is consistent with (3.61) and the estimates in Table III. Similarly, in (3.62d) we can drop the $q_i C_{g_i u}$ term and eliminate $C_{\rho u}$ in favor of C_{uu} , using (3.64), to obtain

TABLE II. Summary of the divergent quantities, and equation numbers of detailed expressions for them.

Quantity	Divergence	Full expression
Elastic "constants"		
$A_R(\vec{q}), B_R(\vec{q}), C_R(\vec{q})$	$(\ln q)^{-4/5}$	(2.30)
$K_{1R}(\vec{q})$	$(\ln q)^{2/5}$	(2.30)
Viscosities		
$\eta_1, \eta_2, \eta_4, \eta_5$	$\omega^{-1}(\ln q)^{-9/5}, \omega \gg q_z(\kappa B/\rho_0)^{1/2}$ $q_z^{-1}(\ln q)^{-9/5}, \omega \ll q_z(\kappa B/\rho_0)^{1/2}$	(1.1), (4.14), and (4.23)
η_3	$(\ln q)^{2s^{2/5}}$	(4.36)
Miscellaneous		
$a_1(q), a_2(q), a_4(q), a_5(q)$	$(\ln q)^{-8/5}$	

$$(z + i\nu_2)C_{g_z u} + i\rho_0(\tilde{\chi}^{-1})_{uu}C_{uu} = 0, \quad (3.65)$$

where we have identified

$$\rho_0(\tilde{\chi}^{-1})_{uu} = k_B T(\chi^{-1})_{uu}. \quad (3.66)$$

Combining (3.65) and (3.62b) leads to the results

$$C_{uu}(\vec{q}, z) = \frac{(z + i\nu_2)}{D} \chi_{uu}, \quad (3.67)$$

where

$$C_{g_z u}(\vec{q}, z) = \frac{-i}{D}, \quad (3.68)$$

$$D = (z - z_+)(z - z_-), \quad (3.69)$$

and

$$z_{\pm} = i\nu_2/2 \pm [(\tilde{\chi}_{uu})^{-1} - (\nu_2/2)^2]^{1/2}. \quad (3.70)$$

C_{pu} can then be evaluated by inserting (3.67) into (3.64). Since $D \sim O(\epsilon^4)$ and $\chi_{uu} \sim O(\epsilon^{-4})$ we easily verify that the estimates in Table II are all consistent. It is not difficult to invert the Laplace transform for $C_{uu}(q, z)$ to find, in this limit, that

$$C_{uu}(\vec{q}, t) = \frac{\beta^{-1}}{(z_+ - z_-)\rho_0} \sum_{\mu=\pm} \frac{\mu e^{-iz_{\mu}t}}{z_{\mu}}. \quad (3.71)$$

D. Dynamic nonlinear contributions

We are now interested in the corrections to the quasilinear approximation due to the dynamical part of the memory function $M^{(c)}(\vec{q}, z)$ defined by (3.54) and (3.52). It is important to point out that if there were no nonlinear terms in the equations of motion, the dynamical part of the memory function would vanish. To see this let us write

$$I_i(\psi) = I_i^N(\psi) + I_i^L(\psi), \quad (3.72)$$

where $I_i^N(\psi)$ contains all nonlinear contributions to $I_i(\psi)$. Inserting (3.72) into (3.52) we find that any terms constant or linear in ψ cancel and we can replace I_i and I_j^{\dagger} in (3.52) with the nonlinear contributions I_i^N and $I_j^{N\dagger}$. If there were

no nonlinear couplings then we would have $M^{(c)}(z) = 0$.

Let us now restrict ourselves to the specific case of smectics *A*. Note, since there are no nonlinear corrections to the continuity equation, that

$$K_{\rho\alpha}^{(c)}(\vec{q}, z) = K_{\alpha\rho}^{(c)}(\vec{q}, z) = 0 \quad (3.73)$$

for any α .

In the quasilinear approximation the damping of the u variable in its equation of motion is proportional to $\Gamma(\chi^{-1})_{uu}$. It is easy to see that within the memory function formalism the correction to this is

$$i\beta M_{uu}^{(c)} = i\beta K_{u\alpha}^{(c)}(\chi^{-1})_{\alpha u} = i\beta K_{uu}^{(c)}(\chi^{-1})_{uu} \quad (3.74)$$

and therefore the renormalized Γ is given by

$$\Gamma_R(\vec{q}, z) = \Gamma + i\rho_0\beta K_{uu}^{(c)}(\vec{q}, z). \quad (3.75)$$

Similarly, we see that $K_{g_i g_j}^{(c)}(\vec{q}, z)$ is to be identified with the nonlinear contribution to the viscosity matrix:

$$L_{g_i g_j}^{(c)}(\vec{q}, z) = L_{g_i g_j}^{(c)}(\vec{q}) + i\beta K_{g_i g_j}^{(c)}(\vec{q}, z)\rho_0^{-1}. \quad (3.76)$$

Finally, we have the contributions $K_{ug_j}^{(c)}(\vec{q}, z)$ and $K_{g_i u}^{(c)}(\vec{q}, z)$. $K_{ug_i}^{(c)}(\vec{q}, z)$ corresponds to a damping term in the u equation linear in g , while $K_{g_i u}^{(c)}(\vec{q}, z)$ leads to a damping term in the g equation linear in u . These damping terms, which do not appear in the linear equations of motion, are not important since they are of higher order in wave number than the leading hydrodynamical results.

We shall calculate $M_{\alpha\beta}^{(c)}(q, z)$ in a perturbation theory in the temperature. The systematics of higher-order corrections in this expansion are complicated and will be discussed in Sec. IV. The calculation of $M_{\alpha\beta}^{(c)}(q, z)$ to lowest order in the temperature, however, is straightforward. This is because fluctuations are small in the low-temperature limit and the probability distribution is effectively Gaussian. The average over a Gaussian probability distribution $P_0[\psi]$ of a product of $2N$ fields ψ will factorize into a sum of products of N two-point correlation functions each of which is proportional to $k_B T$. The essentials of this argument are not changed in the dynamic case although the specific analytic properties of the time-

dependent correlation functions are rather more involved. In the end, the lowest-order contribution to $M^{(c)}$ (and $K^{(c)}$) will come from keeping as few powers of ψ as possible in I_i^N . Thus the lowest-order nonlinear vertex is of the form

$$I_{i,0}^N(\psi) = V_{ijk} \delta(\psi_j \psi_k) \quad (3.77)$$

and we immediately obtain from (3.52), after noting that the “subtraction terms” can be ignored since $\langle I_i^N R(z) \delta_i \psi \rangle_0$ is zero to this order, that

$$K_{ij,0}^{(c)}(z) = i \int_0^{+\infty} dt e^{izt} V_{ilm} V_{jkn}^\dagger \times \langle \delta(\psi_k \psi_n) e^{\tilde{D}_0^\dagger \psi} \delta(\psi_l \psi_m) \rangle_0, \quad (3.78)$$

where the angular brackets with subscript zero indicate a Gaussian average. It is not difficult to show that the Gaussian average factorizes into products of zeroth-order correlation functions such that

$$K_{ij,0}^{(c)}(z) = i \int_0^{+\infty} dt e^{izt} V_{ilm} V_{jkn}^\dagger \times [C_{nm}^0(t) C_{kl}(t) + C_{km}^0(t) C_{nl}^0(t)]. \quad (3.79)$$

We analyze these contributions in detail in Sec. IV.

E. Extension to hexatics-B

The equations of motion³⁸ for hexatics-B are again given by the Langevin equation (3.1) with two modifications: the ψ 's now include ϕ as well as u , \vec{g} , and ρ , and the appropriate Hamiltonian is now (2.32). We also need the Poisson brackets between ϕ and the other variables:

$$\{g_i(\vec{x}), \phi(\vec{x}')\} = \frac{1}{2} \epsilon_{ij} \nabla_j \delta(\vec{x} - \vec{x}'), \quad (3.80a)$$

$$\{u(\vec{x}), \phi(\vec{x}')\} = 0. \quad (3.80b)$$

The linearized version of the resultant equations of motion read, after Fourier-transforming in space,

$$\begin{aligned} \frac{\partial \vec{g}_\perp}{\partial t} + (\eta_2 q_\perp^2 + \eta_3 q_z^2) \vec{g}_\perp + \eta_4 \vec{q}_\perp (\vec{q}_\perp \cdot \vec{g}_\perp) + iA \vec{q}_\perp \rho \\ + (\eta_3 + \eta_5) q_z \vec{q}_\perp g_z - C q_z \vec{q}_\perp u + iz \times \vec{q}_\perp K(q) \phi = \vec{\xi}_\perp, \end{aligned} \quad (3.81a)$$

$$\begin{aligned} \frac{\partial g_z}{\partial t} + i(A - C) q_z \rho + (\eta_3 q_\perp^2 + \eta_1 q_z^2) g_z \\ + (\eta_3 + \eta_5) q_z (\vec{q}_\perp \cdot \vec{g}_\perp) + [(B - C) q_z^2 + K_1 q_\perp^4] u = \xi_z, \end{aligned} \quad (3.81b)$$

$$\frac{\partial u}{\partial t} - \frac{g_z}{\rho} + \Gamma(B q_z^2 + K_1 q_\perp^4) u - i\Gamma C q_z \rho = \theta, \quad (3.81c)$$

$$\frac{\partial \phi}{\partial t} - \frac{1}{2} \hat{z} \cdot (\vec{q}_\perp \times \vec{g}_\perp) + \Gamma_\phi K(q) \phi = \gamma, \quad (3.81d)$$

where $K(\vec{q}) = K_1 q_\perp^2 + K_2 q_z^2$, and we have neglected the irrelevant \vec{g} and g_z terms in the Hamiltonian (2.32). $\gamma(\vec{x}, t)$ is the Gaussian noise for ϕ with correlations:

$$\langle \gamma(\vec{x}, t) \gamma(\vec{x}', t') \rangle = 2k_B T \Gamma_\phi \delta(\vec{x} - \vec{x}') \delta(t - t'), \quad (3.82a)$$

$$\langle \gamma(\vec{x}, t) \xi_i(\vec{x}', t') \rangle = \langle \gamma(\vec{x}, t) \theta(\vec{x}', t') \rangle = 0. \quad (3.82b)$$

The most important feature of these equations for our purposes is that the variables $g_\perp \equiv \vec{q}_\perp \cdot \vec{g}_\perp / q_\perp$, g_z , and u , completely decouple, for all wave vectors \vec{q} , from the variables $g_T \equiv \hat{z} \cdot (\vec{q} \times \vec{g}_\perp)$ and ϕ as can be seen by forming the dot and cross products of (3.81) with \vec{q}_\perp and noting that g_T does not appear in the equations of motion for ρ , u , and g_z . Thus the quasilinearized correlation functions of the variables g_\perp , g_z , ρ , and u are exactly the same as in a smectic-A. In particular, the C_{uu} correlation function is unchanged. Since the nonlinear terms in u in the equations of motion are also identical with those of a smectic-A, all of the divergences derived for that case will also be present here, in precisely the same form. Furthermore, we can show by power counting that the g_T and ϕ fluctuations, when nonlinearly coupled back into the others, give rise to no new divergences.³⁸ This completes the verification of the claim in the Introduction that the smectic-A results transcribe perfectly in hexatics-B.

IV. ANALYSIS OF THE DOMINANT NONLINEAR CONTRIBUTIONS TO THE TRANSPORT COEFFICIENTS

A. Lowest-order contributions

Our first task is the explicit evaluation of the zeroth-order contribution to the dynamic part of the memory function given by (3.51) and (3.79). Given the large number of components and the various integrations involved even this is a formidable task. Fortunately, we can show that the dominant contributions to K^c come from the “streaming terms” quadratic in u . This result follows straightforwardly from the power counting developed in Sec. III C and summarized in Table III. Thus we need only consider a few terms in the streaming velocity, namely,

$$\begin{aligned} V_g^i = \frac{1}{2} (B \delta_{iz} \nabla_z - C \nabla_i) (\vec{\nabla} u)^2 + B \delta_{iz} \vec{\nabla} \cdot (\nabla_z u \vec{\nabla} u) \\ + B \nabla_z (\nabla_i u \nabla_z u) \end{aligned} \quad (4.1)$$

and

$$V_u = \frac{1}{2} \Gamma B \nabla_z (\vec{\nabla} u)^2, \quad (4.2)$$

TABLE III. Summary of power counting for correlation functions and propagators, in the regime of wave vector and frequency $q_\perp \sim O(\epsilon)$, $q_z \sim O(\epsilon^2)$, $\omega \sim O(\epsilon^2)$, and $\epsilon \rightarrow 0$. Top half gives power counting for correlation functions, bottom half for propagator $G_{\alpha\beta}$ with columns as α and rows as β .

	u	ρ	g_3	g_T
u	ϵ^{-6}	ϵ^{-4}	ϵ^{-4}	ϵ^{-2}
ρ	ϵ^{-4}	ϵ^{-2}	ϵ^{-2}	1
g_3	ϵ^{-4}	ϵ^{-2}	ϵ^{-2}	1
g_T	ϵ^{-2}	1	1	ϵ^2
u	ϵ^{-2}	1	1	ϵ^{-1}
ρ	ϵ^{-2}	1	1	ϵ^{-1}
g_3	ϵ^{-4}	ϵ^{-2}	ϵ^{-2}	ϵ^{-3}
g_T	ϵ^{-3}	ϵ^{-1}	ϵ^{-1}	1

where only the relevant parts of each term have been written out. When Fourier-transformed in space, these are

$$V_{gi}(\vec{q}) = \int \frac{d^3p}{(2\pi)^3} V_{giuu}(\vec{q}, \vec{p}) u(\vec{p}) u(\vec{q} - \vec{p}) \quad (4.3)$$

and

$$V_u(\vec{q}) = \int \frac{d^3p}{(2\pi)^3} V_{uuu}(\vec{q}, \vec{p}) u(\vec{q} - \vec{p}) u(\vec{p}), \quad (4.4)$$

where the vertices, corresponding to the V_{ijk} in (3.77), are given by³⁹

$$\begin{aligned} V_{giuu}(\vec{q}, \vec{p}) &\equiv \Gamma_i(\vec{q}, \vec{p}) \\ &= -\frac{i}{2} (Bq_z \delta_{iz} - Cq_i) p^2 + iBq_z p_i p_z \\ &\quad + iB\delta_{iz} p_z \vec{q} \cdot \vec{p}, \end{aligned} \quad (4.5)$$

$$V_{uuu}(\vec{q}, \vec{p}) \equiv \Gamma_u(\vec{q}, \vec{p}) = -\frac{i}{2} \Gamma Bq_z p^2. \quad (4.6)$$

Using these results in (3.79) we find, using (3.74) and (3.75), that the real part of the viscosity matrix is altered by an amount

$$\begin{aligned} \Delta L_{ij}^R(\vec{q}, \omega) &= \text{Re} \beta \rho_0^{-1} K_{gi,0}^{(c)}(\vec{q}, \omega) \\ &= \beta \rho_0^{-1} \int \frac{d^3p}{(2\pi)^3} \frac{d\Omega}{2\pi} \Gamma_i(\vec{q}, \vec{p}) C_{uu}''(\vec{q} - \vec{p}, \omega - \Omega) \\ &\quad \times C_{uu}''(\vec{p}, \Omega) \Gamma_j(-\vec{q}, \vec{p}) \end{aligned} \quad (4.7)$$

while the kinetic coefficient Γ is shifted by

$$\begin{aligned} \Delta \Gamma(\vec{q}, \omega) &= \text{Re} \beta K_{uu,0}^{(c)}(\vec{q}, \omega) \\ &= \int \frac{d^3p}{(2\pi)^3} \frac{d\Omega}{2\pi} \Gamma_u(\vec{q}, \vec{p}) C_{uu}''(\vec{q} - \vec{p}, \omega - \Omega) \\ &\quad \times C_{uu}''(\vec{p}, \Omega) \Gamma_u(-\vec{q}, \vec{p}). \end{aligned} \quad (4.8)$$

In (4.7) and (4.8) $C_{uu}''(\vec{q}, \omega)$ is the Fourier transform over time of $C_{uu}(\vec{q}, t)$ given by (3.71). After inserting the explicit expressions for the vertices given by (4.5) and (4.6) we find that

$$\Delta L_{ij}^R(\vec{q}, \omega) = (B\delta_{iz} q_z - Cq_i)(B\delta_{jz} q_z - Cq_j) I(\vec{q}, \omega) \quad (4.9)$$

and

$$\Delta \Gamma(\vec{q}, \omega) = \Gamma^2 B^2 q_z^2 I(\vec{q}, \omega) \rho_0, \quad (4.10)$$

where

$$\begin{aligned} I(\vec{q}, \omega) &= \frac{\rho_0^{-1}}{4k_B T} \int \frac{d^3p}{(2\pi)^3} \frac{d\Omega}{2\pi} p_1^4 C_{uu}''(\vec{q} - \vec{p}, \omega - \Omega) C_{uu}''(\vec{p}, \Omega). \end{aligned} \quad (4.11)$$

We can then read off the corrections $\Delta\eta_i$ for the individual viscosities from (4.9) using (3.15);

$$\Delta\eta_1 = (B - C)^2 I(\vec{q}, \omega), \quad (4.12a)$$

$$\Delta\eta_4 = C^2 I(\vec{q}, \omega), \quad (4.12b)$$

$$\Delta\eta_5 = C(C - B) I(\vec{q}, \omega). \quad (4.12c)$$

Note that these $\Delta\eta_i$ satisfy

$$\Delta\eta_1 \Delta\eta_4 = (\Delta\eta_5)^2. \quad (4.13)$$

Using the Fourier transform of (3.71) we can carry out the integrals in (4.11) and find that $I(q, \omega)$ diverges as q and ω go to zero. We can gain an understanding of the dependence of $I(q, \omega)$ on \vec{q} and ω in this divergent regime by investigating the extreme cases (a) $\omega \neq 0$, $\vec{q} = 0$; (b) $\omega = 0$, $q_z \gg \lambda q^2 = 0$; and (c) $\omega = 0$, $q_z \ll \lambda q^2$. The analysis is simplified in the limit $\kappa \equiv K_1/\rho_0 \eta_3^2 \ll 1$. [For typical smectics (see Table I) $\kappa \sim 10^{-4}$.] In order to understand the significance for the $\kappa \ll 1$ limit, note that η_3 governs the damping of the undulation mode parallel to the layers, and K_1 its speed in that direction. Analysis of the normal modes of the $u-u$ correlation function, given by (3.70), show that for $\kappa < \frac{1}{4}$ the undulation mode is diffusive for $q_z = 0$. More importantly, for $\kappa \rightarrow 0$ and $q_z \leq \lambda q^2$, the eigenfrequencies z_{\pm} of the undulation mode satisfy $z_{+} \sim \kappa z_{-} \ll z_{-}$. Thus only the contribution from the single mode with frequency z_{+} needs to be taken into account. This fact simplifies the evaluation of $I(\vec{q}, \omega)$ in the cases mentioned above. We find that in d dimensions $I(\vec{0}, \omega) \sim \omega^{(d-5)/2}$, $I(q_z, 0) \sim q_z^{(d-5)/2}$, and $I(\vec{q}_{\perp}, 0) \sim |\vec{q}_{\perp}|^{d-5}$. In more detail, for $d = 3$,

$$I(\vec{0}, \omega) = \frac{w}{64B'\rho_0} \frac{1}{\omega}, \quad (4.14a)$$

$$I(q_z, 0) = \frac{(\pi - 2)w\eta_3}{64\pi(B')^2} \frac{1}{\lambda q_z}, \quad (4.14b)$$

$$I(\vec{q}_{\perp}, 0) \sim q_{\perp}^{-2}. \quad (4.14c)$$

This means, with the use of (4.10), that

$$\Delta\Gamma \sim \begin{cases} q_z^2/|\omega| & \text{for } |\omega| \gg |\vec{q}| \\ q_z & \text{for } \omega = 0, q_z \gg \lambda q_{\perp}^2 \\ q_z/\lambda q_{\perp}^2 & \text{for } \omega = 0, q_z \ll \lambda q_{\perp}^2 \end{cases} \quad (4.15a)$$

$$\Delta\Gamma \sim \begin{cases} q_z^2/|\omega| & \text{for } |\omega| \gg |\vec{q}| \\ q_z & \text{for } \omega = 0, q_z \gg \lambda q_{\perp}^2 \\ q_z/\lambda q_{\perp}^2 & \text{for } \omega = 0, q_z \ll \lambda q_{\perp}^2 \end{cases} \quad (4.15b)$$

$$\Delta\Gamma \sim \begin{cases} q_z^2/|\omega| & \text{for } |\omega| \gg |\vec{q}| \\ q_z & \text{for } \omega = 0, q_z \gg \lambda q_{\perp}^2 \\ q_z/\lambda q_{\perp}^2 & \text{for } \omega = 0, q_z \ll \lambda q_{\perp}^2 \end{cases} \quad (4.15c)$$

All the above corrections vanish for $q \rightarrow 0$ so that Γ is unaffected at long wavelengths by the nonlinearities. The viscosities η_1 , η_4 , and η_5 diverge as $1/\omega$ for very long wavelength probes as seen from (4.12).

A particularly useful way of looking for transport anomalies in these systems is through a study of the sound attenuations. The sound attenuations $\alpha_i(\theta, \omega)$ are related to the renormalized elastic constants and transport coefficients by (3.60). Thus, to obtain the shift in $\alpha_i(\theta, \omega)$ due to the nonlinearities, we simply replace the η_i 's and Γ in (3.60) by their shifted values. As shown above $\Delta\Gamma$ makes a negligible change, but the shifts in the viscosities, $\Delta\eta_i$, lead to a significant shift, $\Delta\alpha_i(\theta, \omega)$, in the sound attenuation. Notice that in evaluating $\Delta\alpha_i$ we must evaluate $\Delta\eta_i$, and therefore $I(\vec{q}, \omega)$, for wave numbers and frequencies satisfying the dispersion relation $q_i = \omega/c_i$ [see (1.31)]. Thus we need to evaluate $I(\omega/c_i, \omega)$ in order to obtain the nonlinear contributions to the sound attenuation. Note,

however, from (4.14), that

$$\frac{I(\vec{0}, \omega)}{I(\vec{q}_\perp, 0)} \sim \frac{q_\perp^2}{\omega} \sim \frac{\omega}{c_i}, \quad (4.16a)$$

$$\frac{I(\vec{0}, \omega)}{I(q_z, 0)} \sim \sqrt{\kappa} \left[\frac{B'}{\rho_0} \right]^{1/2} \frac{q_z}{\omega} \sim \left[\frac{B'\kappa}{\rho_0} \right]^{1/2} \frac{1}{c_i}, \quad (4.16b)$$

and in both cases, except for the case of second sound propagating almost along the ordering direction, we have $I(\vec{q}, 0) \gg I(\vec{0}, \omega)$, since $\kappa \ll 1$. This means that the frequency provides a cutoff at a shorter spatial scale than q and the additional cutoff due to q is negligible. Therefore, to a very good approximation

$$I(\omega/c_i, \omega) \cong I(0, \omega) \quad (4.17)$$

except for propagation of second sound almost along the ordering direction. In this case c_2 vanishes and $I(\vec{0}, \omega)$ can no longer be taken as small in comparison with $I(q_z, 0)$. A detailed analysis shows that ω is the relevant cutoff until q_\perp/q_z is less than $\sqrt{\kappa}$ which is on the order of 0.01. We have then that the attenuations go as ω for second sound except when it propagates at an angle of less than 10^{-2} rad ($\frac{1}{2}$ deg) to the layer normal. In that case we expect the attenuation to diverge as I/q_z . The resolution available in experiments is, however, of the order of a few degrees so this effect is probably not observable.

The case of second sound in the layers, i.e., $q_z \ll \lambda q^2$, is different, since the damping here is governed [(3.60) for $\theta \approx \pi/2$] entirely by η_3 . This viscosity diverges only logarithmically, as we shall show in Sec. IV D, so that $I(\vec{q}, \omega)$ does not enter, and the anomaly in this range of wave vectors is a very mild one. It should be noted that η_3 is the only viscosity appearing in $I(\vec{q}, \omega)$. The fact that it suffers no power-law divergences implies that the perturbation theory is self-consistent to this order, apart from logarithmic corrections. We shall now show that the $1/\omega$ (or $1/q_z$) nature of the anomaly as well as the relation (4.13) hold to all orders.

B. Higher-order corrections

Since the lowest-order corrections to the viscosities are divergently larger than the bare viscosities, the validity of the entire perturbation theory might seem dubious. Indeed, in other situations, such as critical phenomena, the true divergences can only be obtained by either cleverly resumming an infinite series of such individually divergent terms, or by performing an expansion around the upper critical dimension (5 in this case) below which the divergences occur. Fortunately, such an approach is not necessary; the divergences at higher order are no worse than $1/\omega$, and we can say with confidence that the physical viscosities do indeed diverge like $1/\omega$.

In order to show this we must develop a systematic approach to the calculation of higher-order corrections to the memory function. This is most conveniently (for the pictorially minded) done with the use of the graphical approach described by Ma and Mazenko.³¹ We begin by graphically representing the equations of motion as illustrated in Fig. 4. This representation suggests a straight-

$$a \Rightarrow = a \rightarrow \circ + a \rightarrow \text{vertex} + \dots$$

FIG. 4. Graphical representation of the equation of motion. Thick lines represent the fluctuating fields; thin ones, the bare propagators [defined by Eq. (3.4)] evaluated in the quasilinear approximation. Points where n fields meet represent n th order nonlinear terms (vertices) in the equations of motion, and the small circles represent the Langevin noises. Sums over repeated indices, which include frequency and wave vectors as well as field labels are implied.

forward iterative solution, obtained by replacing each of the ψ lines in the nonlinear vertices, by the expression for ψ itself. This leads to the iterated form represented graphically in Fig. 5. Note that to solve the equations to n th order in the external noise (which amounts, as we shall see, to calculating the correlation functions to n th order in temperature) we need only include such “tree” graphs of no more than $n + 1$ branches.

Now consider the calculation of correlation functions. The thermal averaging that must be performed in such a calculation involves, in the Langevin-equation approach used here, an average over the external noises. Because the latter are Gaussian, averages over products of several such noises can be replaced by products of averages of pairs of noises. This pairwise averaging can be represented by joining the branches in the iterative solutions to the equations of motion at the noise bubbles, as illustrated in Fig. 6. A single such pairing [(a) of Fig. 6] gives the quasilinear correlation function $C_{\alpha\beta}^0$. These graphs now have all the properties of Feynman diagrams; momentum and frequency are conserved (by construction at the vertices, and as a result of the δ -function correlations of the noises through the correlation lines) and integrals over all unconstrained loop wave vectors \vec{p} and frequencies Ω are implied.

We can now apply this graphical procedure to the calculation of any correlation function. In particular, we can calculate the various correlation functions contributing to the dynamical memory function $M_{\alpha\beta}^{(c)}$ given by (3.52). Since the second term on the right in (3.52) acts to remove various one-body reducible terms from the first term, we can take it into account by considering only the irreducible graphs contributing to the first term in (3.52). We compute then the contribution of irreducible graphs to the imaginary part of $\langle I_j^\dagger R(z) I_i \rangle$, which gives the higher-order corrections to the transport coefficients. Two of the graphs that result are shown explicitly in (b) and (c) of Fig. 6. Higher-order corrections are shown in Figs. 7 and 8. Figure 7(b), with the internal indices all set to u ,

$$a \Rightarrow = a \rightarrow \circ + a \rightarrow \text{vertex} \rightarrow \text{vertex} \rightarrow \dots$$

FIG. 5. Graphical representation of the iterative solution of the equations of motion. Note that each “branch” of every “tree” ultimately terminates on a noise.

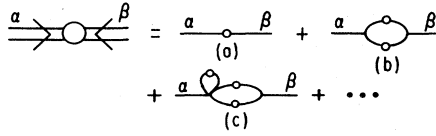


FIG. 6. Graphs for the correlation function $C_{\alpha\beta}$. Note that we can "tie legs together" either by correlating noises between the two fields (α, β) being correlated, as in (a) and (b), or correlating them within the noises for each, as in the ear of (c). Note also that tying together just two legs generates the quasilinear approximation for the correlation function $C_{\alpha\beta}^0$.

represents the lowest-order correction to the viscosity tensor and was analyzed in detail in the first part of this section. There are two classes of higher-order diagrams, illustrated in Figs. 7 and 8, whose contribution to the viscosity tensor also diverge as $1/\omega$ at low frequencies. The first class, illustrated in Fig. 7, arise from vertices involving four u legs⁴⁰ [see Figs. 7(a) and 7(b)] or six or more u legs⁴¹ [see Fig. 7(c)] in the equation of motion for g . Graphs arising from such vertices in which none of the legs are diverted into "ears,"⁴² can be shown by power counting to diverge, at most, logarithmically. We can include any graphs in which all the "extra" legs (i.e., all but two of them for a higher than three point vertex) are diverted into a subsidiary ear by replacing every three-point vertex with a renormalized three-point vertex,⁴³ given graphically in Fig. 9. This renormalized vertex differs in three important ways from the original or bare one.

(1) It is not expressible, even in principle, in terms of the elastic constants A_R , B_R , and C_R , but requires the introduction of new phenomenological parameters which depend on the microscopic (short-distance) details of the system.

(2) Its tensor structure is different. As we shall see, this leads to the $1/\omega$ divergence of the shear viscosity η_2 .

(3) It is temperature dependent. All the corrections to the bare three-point vertex are higher order in temperature, since they involve one or more loops, and hence van-

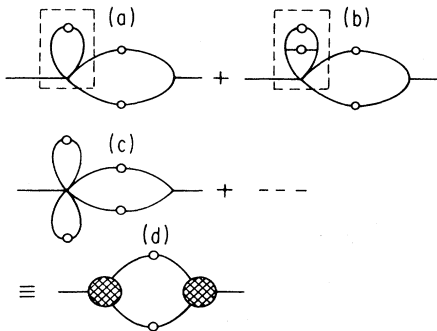


FIG. 7. Graphs for $K_{\alpha\beta}$ arising from higher-order vertices in the equations of motion that also diverge as $1/\omega$ at small ω . "Ears" described in the text are inside the dotted lines, and can be absorbed into a renormalized three-point vertex as illustrated here and in Fig. 8.

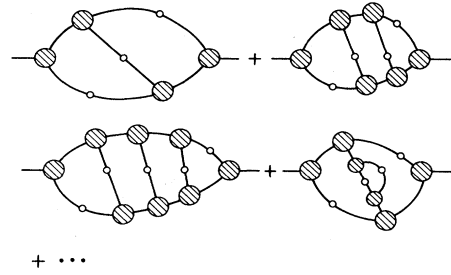


FIG. 8. Higher-order corrections that cannot be absorbed into the renormalized three-point vertex. None of them diverge more strongly than $1/\omega$.

ish as $T \rightarrow 0$. Consequently, the results of Ref. 1 and the beginning of this section are recovered in the low-temperature limit.

Statements (1) and (2) are apparent even at one-loop order. Evaluating the first and second graphs in Fig. 9 we find the renormalized vertices are

$$\begin{aligned} \Gamma_i^R(\vec{q}, \vec{p}) &= \Gamma_i(\vec{q}, \vec{p}) \\ &\quad - iB \left[\frac{3}{2} b \delta_{iz} q_z p^2 + 2d q_i p^2 \right. \\ &\quad \left. - 4d (q_z p_i p_z + \delta_{iz} p_z \vec{q} \cdot \vec{p} + p_i \vec{q} \cdot \vec{p}) \right], \end{aligned} \quad (4.18)$$

where Γ_i is given by (4.5) and

$$d = \frac{1}{2} \langle (\vec{\nabla}_\perp u)^2 \rangle, \quad (4.19a)$$

$$b = \frac{1}{2} \langle (\nabla_z u)^2 \rangle - d. \quad (4.19b)$$

The new tensor structure of Γ_i^R , relative to Γ_i^0 , is reflected in the term proportional to $p_i \vec{q} \cdot \vec{p}$. This corresponds to a nonlinearity proportional to $\vec{\nabla} \cdot (\nabla_i u \vec{\nabla} u)$ and is not present in the bare vertex. As we shall see later this new term is responsible for the divergence of the shear viscosity η_2 .

The statement above that this vertex involves new phenomenological parameters becomes apparent when we actually attempt to evaluate d and b given by (4.19). We have that

$$\begin{aligned} d &= \int \frac{d^3 q}{(2\pi)^3} (\vec{q}_\perp)^2 \chi_{uu}(\vec{q}) \\ &= k_B T \int \frac{d^3 q (\vec{q}_\perp)^2}{(2\pi)^3 [B_R'(\vec{q}) q_z^2 + K_{1R}(\vec{q}) q^4]} \end{aligned} \quad (4.20a)$$

and

$$b + d = \int \frac{d^3 q}{(2\pi)^3} q_z^2 \chi_{uu}(\vec{q}), \quad (4.20b)$$

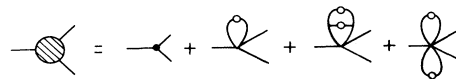


FIG. 9. Graphs for the renormalized three-point vertex.

where $B'_R(\vec{q})$ and $K_{1R}(\vec{q})$ depend logarithmically on \vec{q} , as given in (2.30). Both of these integrals diverge for large \vec{q} . This divergence is merely an artifact of our truncation of the gradient expansion of the Hamiltonian (2.2) at lowest order in the gradients. The inclusion of higher gradients [e.g., a $(\nabla^4 u)^2$ term] in this expansion would render d and b finite. The coefficients of these higher-order terms, however, are new phenomenological parameters, which are not determined by those already introduced. Hence we suffer no loss of information if we simply consider d and b themselves to be new adjustable, temperature-dependent parameters.

We can estimate the order of magnitude of d and b by simply restricting the domain of integration in (4.20) to a cylindrical Brillouin zone with $|\vec{q}_\perp| < \Lambda_\perp$, $|q_z| < \Lambda_z \gg \Lambda_\perp$. We have then from (4.20) that

$$d \cong \frac{k_B T \Lambda_\perp^2}{8\pi(B_R K_{1R})^{1/2}}, \quad (4.21a)$$

$$b = \frac{k_B T}{8\pi^2 B_R} \Lambda_z \Lambda_\perp^2. \quad (4.21b)$$

If we assume that Λ_\perp is of the order of magnitude of the layering wave number $q_0 = 2\pi/a$ and insert typical values for monolayer smectic at a temperature of 350 K, we find $d \approx 0.06$. Looking at the renormalized vertex we find a first-order correction to the coefficient of $q_i p^2$ of roughly $0.12B$. Since the "bare" value of this coefficient is $C/2$, which typically is $\sim B/6$, we see that the correction is quite large. We must emphasize that our estimates for d and b above are very crude. We do not really know how to treat the wave-number cutoffs accurately.

An important question at this point is whether new vertex terms will be generated at higher order to correct (4.18) just as $\vec{\nabla} \cdot (\nabla_i u \vec{\nabla} u)$ was generated at first order. This question can be answered by constructing the most general vertex compatible with the symmetries of the system. These are the following:

(i) the symmetry of the stress tensor and conservation of momentum, which imply that $\Gamma_i^R(\vec{q}, \vec{p}) = q_j A_{ij}(\vec{q}, \vec{p})$ where A_{ij} is symmetric;

(ii) translation invariance, which requires that only gradients of u appear, so that (since Γ_i^R couples to a pair of u 's) A_{ij} must be quadratic in \vec{q} and \vec{p} ; and

(iii) uniaxiality.

Taken together, these lead, apart from irrelevant terms, to the form

$$\begin{aligned} \Gamma_i^R(\vec{q}, \vec{p}) = & -\frac{i}{2} [\tilde{B} \delta_{iz} q_z p^2 - \tilde{C} p_i p^2 + \gamma p_i \vec{q} \cdot \vec{p} \\ & + \mu(p_i q_z p_z + \delta_{iz} p_z \vec{q} \cdot \vec{p})]. \end{aligned} \quad (4.22)$$

We note immediately that no new types of terms can be generated beyond those already present in the first-order result (4.18). It is equally important to realize that the coefficients \tilde{B} , \tilde{C} , γ , and μ appearing in (4.22) are simply

related to previously determined parameters *only* at zeroth order. Even at first order the parameters \tilde{B} , \tilde{C} , γ , and μ depend on the short-distance properties of the system and should, within a hydrodynamic development, be taken as independent, adjustable parameters.

If we analyze the contribution of the graph shown in Fig. 7(d) to the viscosity matrix using the general vertex (4.22) we find that the four viscosities η_1 , η_2 , η_4 , and η_5 diverge as $1/\omega$. Their divergent parts are given by

$$\delta\eta_1 = (\tilde{B} - \tilde{C})^2 I(\vec{q}, \omega), \quad (4.23a)$$

$$\delta\eta_2 = \gamma^2 I(\vec{q}, \omega) / 8, \quad (4.23b)$$

$$\delta\eta_4 = (\tilde{C} - \gamma/2)^2 I(\vec{q}, \omega), \quad (4.23c)$$

$$\delta\eta_5 = (\tilde{C} - \tilde{B})(\tilde{C} - \gamma/2) I(\vec{q}, \omega). \quad (4.23d)$$

Defining

$$a_1 = (\tilde{B} - \tilde{C})^2, \quad (4.24a)$$

$$a_2 = \gamma^2 / 8, \quad (4.24b)$$

$$a_4 = (\tilde{C} - \gamma/2)^2, \quad (4.24c)$$

and

$$a_5 = (\tilde{C} - \tilde{B})(\tilde{C} - \gamma/2) \quad (4.24d)$$

we recover the results (1.1) and (1.2). The main new qualitative feature of these results when compared with the results reported in I is that the shear viscosity η_2 diverges as $1/\omega$. In particular, for low temperatures, we have, on comparing (4.22) and (4.18), that

$$a_1 = (B - C)^2 + O(T), \quad (4.25a)$$

$$a_2 = O(T^2), \quad (4.25b)$$

$$a_4 = C^2 + O(T), \quad (4.25c)$$

$$a_5 = C(C - B) + O(T), \quad (4.25d)$$

and in the $T \rightarrow 0$ limit we recover the results of I. The most important consequence of higher-order corrections may be to change the sign of a_5 which is negative at low temperatures since $B > C$.

Using these results for the divergent parts of the viscosities in (3.60) for the anomalous part of the sound attenuation we obtain (1.5) with $f_i(\theta)$ given by

$$f_i(\theta) = \frac{(-1)^i}{2\rho_0 c_i^3(\theta)[c_1^2(\theta) - c_2^2(\theta)]} \{ \sin^2\theta \cos^2\theta [a_1 A_R + (a_2 + a_4)(A_R + B_R - 2C_R) + 2a_5(C_R - A_R)] \\ - \rho_0 c_i^2(\theta) [a_1 \cos^2\theta + (a_2 + a_4) \sin^2\theta] \} . \quad (4.26)$$

The higher-order corrections discussed above are, to a large degree, of a static nature. Those depicted in Fig. 8 are essentially dynamical, and arise from the insertion of additional correlation function lines into the divergent bubble. We shall now argue that these graphs also diverge as $1/\omega$, and that no other graphs, at any order, diverge more strongly. To do this, it is useful to first show that any $(n+1)$ -loop graph produced by adding lines to any n -loop graph can diverge no more strongly than the original n -loop graph. The argument is based on simple power counting: The most divergent insertion we can add to a graph is a u - u correlation function which, as shown in Table II, diverges as ϵ^{-6} in the dominant frequency and wave-number regime. The largest such insertion will involve the renormalized three-point vertex Γ^R . In making such an insertion, we also introduce two propagator lines. The largest such propagator (see Table III) is $G_{ug_z} \sim O(\epsilon^{-4})$. Thus the largest correction to the viscosities involves the insertion of two such propagators, and hence two Γ_z^R , which are of $O(\epsilon^4)$.⁴⁴ In addition to these factors, we must, in an $(n+1)$ -loop graph, integrate over one more momentum and frequency (relative to an n -loop graph). Since the width of the regime of frequencies that contributes appreciably is of $O(\epsilon^2)$, the additional integral over frequency contributes a factor of $O(\epsilon^2)$. Likewise, the additional dp_z and d^2p_\perp integrals each contribute a factor of $O(\epsilon^2)$ as well for a net "phase-space" factor of $O(\epsilon^6)$. If we then estimate the value of the first graph in Fig. 8, relative to Fig. 6(b), we obtain a factor of $O(\epsilon^{-6})$ from the additional C_{uu} correlation function, two factors of $O(\epsilon^4)$ from the vertices, two factors of $O(\epsilon^{-4})$ from the two $G_{g_z u}$ propagators and a factor of $O(\epsilon^6)$ from the additional phase-space integration. Multiplying these factors we obtain a contribution of $O(1)$ relative to Fig. 6(b). Similarly, all of the graphs in Fig. 8 are of $O(1)$ relative to Fig. 6(b). Taking all of this information together we find that higher-order graphs diverge, at most, as strongly as the most divergent one-loop graph, i.e., like $1/\omega$. Furthermore, since all of these higher-order graphs are constructed from the same generalized three-point vertex (4.22), they contribute to the viscosity matrix with the same tensor structure as the lowest-order results. This implies that the relation (1.3) continues to hold to all orders of perturbation theory.

C. Logarithmic corrections to viscosities

The dynamic results presented above neglect logarithmic divergences of the static parameters [as given by (2.30), for example], which enter the dynamic calculation, as well as intrinsic dynamic logarithmic divergences. We discuss these corrections here.

We first note that the parameters \tilde{B} , \tilde{C} , γ , and μ , which

enter the renormalized vertex Γ_i^R given by (4.22), all depend on \vec{q} in exactly the same way as in $B_R(\vec{q})$ [or equivalently $C_R(\vec{q})$]. That is, $\tilde{B}_R(\vec{q}) = \tilde{B} B_R(\vec{q}) / B$ [and equivalent expressions for $\tilde{C}_R(\vec{q})$, $\gamma_R(\vec{q})$, and $\mu_R(q)$]. This is readily seen by noting that all contributions to these parameters are proportional either to B or C (including those that come from the vertex corrections discussed earlier) or to coefficients of higher powers of the invariant in the Hamiltonian. The latter are easily shown (by use of the RG constructed in Sec. II) to have the same wave-vector dependence as $B_R(\vec{q})$.

For the four viscosities whose principal divergence is as $1/\omega$ the logarithmic corrections are given accurately by (4.23) provided the vertex parameters \tilde{B} , \tilde{C} , and γ are replaced with the wave-vector-dependent quantities described above. It should be emphasized that these quantities depend only on wave vector, not on frequency, since they are all derivable from static correlation functions.

The one viscosity, η_3 , which does not diverge as $1/\omega$, diverges logarithmically with ω . This divergence comes from Fig. 7 where the vertices are given by the μ terms in the renormalized vertex Γ_i^R . We find that the corresponding correction to the viscosity matrix is

$$\Delta L_{ij}^\mu(\vec{q}, \omega) = \frac{\rho_0^{-1} \mu^2(\vec{q})}{4k_B T} I_2(\vec{q}, \omega) [q_z^2 \delta_{ij} + \delta_{iz} \delta_{jz} (q^2 - 4q_z^2) \\ + q_z (q_i \delta_{jz} + q_j \delta_{iz})] , \quad (4.27)$$

where

$$I_2(\vec{q}, \omega) = \int \frac{d^3p}{(2\pi)^3} \frac{d\Omega}{2\pi} p^2 p_z^2 C_{uu}''(\vec{p}, \Omega) C_{uu}''(\vec{q} - \vec{p}, \omega - \Omega) . \quad (4.28)$$

We readily recognize from (3.15) that ΔL_{ij}^μ is simply a correction to the viscosity η_3 :

$$\Delta \eta_3(\vec{q}, \omega) = \frac{\rho_0^{-1} \mu^2(\vec{q})}{4k_B T} I_2(\vec{q}, \omega) . \quad (4.29)$$

As with $I(\vec{q}, \omega)$ we can evaluate $I_2(\vec{q}, \omega)$ in the small- κ limit. We find

$$\Delta \eta_3(\vec{q}, \omega) = \frac{s^2 \omega}{32\pi} \left[\frac{B(\vec{q})}{B'(\vec{q})} \right]^2 \eta_3 \ln \gamma , \quad (4.30)$$

where

$$\gamma^2 = \begin{cases} (\Lambda^2 K_1 / \rho_0 \eta_3 \omega) & \text{for } (\rho_0 / B')^{1/2} \omega \gg q_z, \lambda q^2 \\ \lambda \Lambda^2 / q_z & \text{for } q_z \gg (\rho_0 / B')^{1/2} \omega, \lambda q^2 \end{cases} \quad (4.31a)$$

$$\gamma^2 = \begin{cases} \lambda \Lambda^2 / q_z & \text{for } q_z \gg (\rho_0 / B')^{1/2} \omega, \lambda q^2 \\ \Lambda^2 / q_z^2 & \text{for } \lambda q^2 \gg q_z, (\rho_0 / B')^{1/2} \omega \end{cases} \quad (4.31b)$$

$$\gamma^2 = \begin{cases} \Lambda^2 / q_z^2 & \text{for } \lambda q^2 \gg q_z, (\rho_0 / B')^{1/2} \omega \end{cases} \quad (4.31c)$$

and

$$s = \mu(\vec{q})/B(\vec{q}) \quad (4.32)$$

is a constant independent of \vec{q} (as discussed above). As in our discussion below (4.16), the first limit (4.31a) applies to propagating sound in all known smectics, except for second sound almost normal to the smectic layers.

Note that unlike the previous expressions for the other viscosities, the variable being renormalized appears on the right-hand side of (4.30). If we are careful then this equation should really be replaced by a self-consistent equation in which the dependence of η_3 (and, for that matter, w) on \vec{q} and ω is taken into account in the evaluation of I_2 . Fortunately, there is a simple way of doing this calculation. The divergence in (4.30) due to $\ln\gamma$ comes from an integral $\int_{\gamma^{-1}} dx/x$. We can think of carrying out this process in such a way that we replace the lower cutoff γ^{-1} with a new cutoff $b^{-1} \equiv e^{-l}$. As in Sec. II, we can then define quantities like $w(l)$, given by (2.22), which correspond to the physical quantity but with all wave numbers restricted to a shell between Λ and Λe^{-l} . We can then carry out a calculation where we change l by an infinitesimal amount δl . It is clear that the change in η_3 can be written as

$$\delta\eta_3(l) = \frac{s^2 w(l)}{32\pi} \left[\frac{B(l)}{B'(l)} \right]^2 \eta_3(l) \int_{e^{-(l+\delta l)}}^{e^{-l}} \frac{dx}{x}, \quad (4.33a)$$

$$= \frac{s^2 w(l)}{32\pi} \left[\frac{B(l)}{B'(l)} \right]^2 \eta_3(l) \delta l. \quad (4.33b)$$

Notice that the l -dependent quantities $w(l)$, $B(l)$, $B'(l)$, and $\eta_3(l)$ enter on the right-hand side since they have been "pulled out" from the integral in (4.33a). We then directly obtain the differential equation

$$\frac{d\eta_3(l)}{dl} = \frac{s^2 w(l)}{32\pi} \left[\frac{B(l)}{B'(l)} \right]^2 \eta_3(l) \quad (4.34)$$

with the boundary condition

$$\eta_3(\vec{q}, \omega) = \eta_3(l = \ln\gamma). \quad (4.35)$$

Since B and B' rarely differ by more than a tenth of a percent we take $B(l)/B'(l) = 1$ in (4.34). Substituting $w(l)$ given by (2.24) in (4.34) we easily solve the resulting differential equation to obtain

$$\eta_3(\vec{q}, \omega) = \eta_3 \left[1 + \frac{5w \ln\gamma}{64\pi} \right]^{2s^2/5} \quad (4.36)$$

and we recall that γ is given as a function of \vec{q} and ω by (4.31). We see that η_3 diverges logarithmically with wave number and frequency with a nonuniversal exponent $2s^2/5$. In the low-temperature limit (where Γ_i^R approaches its bare value) $B \rightarrow B$, $\mu \rightarrow B/2$, and $s = \frac{1}{2}$. Thus the exponent is $\frac{1}{10}$. In general, however, s is another system-dependent parameter.

D. Magnetic field effects

The strong divergence found above for the viscosities at low wave vector and frequency is ultimately a consequence

of the rotational invariance of the smectic- A system. Breaking this symmetry by applying an external magnetic field H (as is routinely done in experiment) will destroy this divergence and all the viscosities will approach finite limits at wave vectors and frequencies $q < q_c = \lambda/\xi_M^2$ and $\omega < \omega_c = \kappa\eta_3/\xi_M^2$ (where ξ_M will be defined below) as in conventional hydrodynamics. To recover our earlier results for the zero-field case, these limiting values must diverge as $H \rightarrow 0$. In this section we calculate these divergences.

The starting point of this discussion is the inclusion³ in the Hamiltonian of the magnetic field energy:

$$F = F_0 + \frac{1}{2} \chi_a \int H^2 |\vec{\nabla}_\perp u|^2 d^3x, \quad (4.37)$$

where χ_a is the anisotropic part of the susceptibility, H is the applied external field, and F_0 is the Hamiltonian (2.2).

The equations of motion (3.1) and the Poisson brackets [(3.9)–(3.11)] are valid quite generally, independently of the precise form of the free energy. Inserting the free energy (4.43) into (3.1), we find that all of our earlier results for the nonlinear terms and the correlation functions still apply, provided we replace the static propagator χ_{uu}^{-1} by

$$(\chi^{-1})_{uu} \rightarrow (\chi^{-1})_{uu} + \chi_a H^2 q_\perp^2. \quad (4.38)$$

With this replacement, we can now evaluate $\delta\eta_i(\vec{q}=0, \omega=0)$ from (4.11) and (4.12). We find for $i=1, 2, 4$, and 5 that

$$\delta\eta_i(\vec{0}, 0) = C_H a_i \eta_3 w \xi_M^2 / 128\pi \lambda^2 (B')^2, \quad (4.39)$$

where $\xi_M^2 = K_1/\chi_a H^2$ and C_H is a temperature-dependent constant⁴⁵ of order unity which approaches 1 as $T \rightarrow 0$. Note that these viscosities diverge as $1/H^2$ as $H \rightarrow 0$. This could be tested in, for instance, smectic- A flow through broad capillaries in strong magnetic fields.

The wave vectors and frequencies at which these magnetic effects become important can be estimated simply by comparing the divergence found above as a function of magnetic field with the corresponding zero-field divergences for frequency ω and wave vector q_z . The crossover between the finite H , ω (or q_z) $\rightarrow 0$ and finite ω (or q_z), $H \rightarrow 0$ limits occur when these are roughly equal. This gives

$$\omega_c(H) = \kappa\eta_3/\xi_M^2 \quad (4.40)$$

for the frequency-field and

$$q_c(H) = \lambda/\xi_M^2 \quad (4.41)$$

for the wave-vector-field crossover, respectively.

V. EXPERIMENTAL CONSEQUENCES

We have already discussed ultrasonic attenuation experiments as tests of the theory presented here. The available ultrasound measurements confirm quite clearly our predictions both for the frequency dependence ($1/\omega$) of the anomaly and the relation (1.3) between the diverging viscosities.

There are, however, several other possible experimental tests. Experiments on the propagation and damping of

second sound (as well as additional data on first sound) at low frequencies are clearly called for in order to test in detail our predictions for the acoustical properties of smectics. Information from these experiments can be compared with our expressions (4.26) for the anomalous attenuation as well as with those of Grinstein and Pelcovits² and the present work for the logarithmic corrections to the elastic moduli. The frequency dependence of the viscosities can also be checked in experiments that measure the impedance of the smectic to ac compression and shear, details of which may be found in, for example, Ref. 21.

The viscosity η_2 determines the viscous stress set up in response to a flow whose direction and gradient are orthogonal, both lying in the smectic layers (Fig. 10). Therefore, the divergent nature of η_2 should be observable when a macroscopic velocity gradient is imposed on a smectic-A by, say, forcing the smectic to flow through a narrow capillary in a suitable geometry. We expect these divergences to manifest themselves in a singular dependence of the viscosity on the flow rate. Such effects come about because the shearing fluid enhances the dissipation of the thermally excited modes which cause the divergence of the viscosity. A flow in the presence of such a viscosity will clearly be non-Newtonian, and non-Newtonian behavior has, in fact, been observed in the decay of pressure in capillary flow experiments on smectics by Kim *et al.*²² and by Bhattacharya and Letcher.²³ A direct mea-

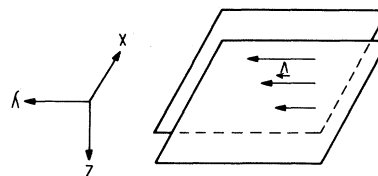


FIG. 10. Geometry of the shear flow experiment discussed in the text. Planes represent the smectic layers.

surement of the relation of viscous stress to strain rate in smectics, as is possible in plane Couette flow experiments, would also be of great interest. A quantitative comparison of experiment with theory in either case awaits a detailed calculation²⁴ which is now in progress.

ACKNOWLEDGMENTS

One of us (G.F.M.) thanks Dr. Geoffrey Grinstein for suggesting this problem and for his comments in the early stages of this research. We thank Dr. Sabyasachi Bhattacharya for many useful discussions and suggestions. G.F.M. and S.R. were supported by National Science Foundation Grant No. DMR-80-20608. J.T. and S.R. were supported by National Science Foundation Material Research Laboratory at The University of Chicago. J.T. was also supported by a grant from Xerox Corporation.

*Present address: Department of Physics, University of Pennsylvania, Philadelphia, Pennsylvania 19174.

†Present address: IBM Thomas J. Watson Research Center, P. O. Box 218, Yorktown Heights, New York 10598.

¹G. F. Mazenko, S. Ramaswamy, and J. Toner, Phys. Rev. Lett. **49**, 51 (1982); referred to as I.

²G. Grinstein and R. Pelcovits, Phys. Rev. Lett. **47**, 856 (1981); Phys. Rev. A **26**, 915 (1982).

³P. G. de Gennes, *The Physics of Liquid Crystals* (Oxford University Press, London, 1974).

⁴R. Pindak, D. E. Moncton, S. C. Davey, and J. W. Goodby, Phys. Rev. Lett. **46**, 1135 (1981).

⁵The materials themselves are, of course, three dimensional; "one dimensional" simply refers to the single direction of inhomogeneity.

⁶P. C. Martin, O. Parodi, and P. S. Pershan, Phys. Rev. A **6**, 2401 (1972).

⁷See, e.g., S. Bhattacharya, B. K. Sarma, and J. B. Ketterson, Phys. Rev. B **23**, 2397 (1981).

⁸See, e.g., B. Y. Cheng, B. K. Sarma, J. D. Calder, S. Bhattacharya, and J. B. Ketterson, Phys. Rev. Lett. **46**, 828 (1981).

⁹See, e.g., N. A. Clark, Phys. Rev. A **14**, 1551 (1976).

¹⁰S. Bhattacharya (private communication).

¹¹P. G. de Gennes, J. Phys. Suppl. **30**, 65 (1969).

¹²York Liao, Noel A. Clark, and P. S. Pershan, Phys. Rev. Lett. **30**, 1047 (1973); K. Miyano and J. B. Ketterson, *ibid.* **31**, 639 (1973).

¹³The low-temperature limit of this result is given incorrectly in I; the coefficient of the $\delta\eta_2$ term in Eq. (14) of that paper

should be $2(C-A)$, not $(C-2A)$. The numerical difference between the two expressions is something less than 0.5%.

¹⁴To make this determination we, of course, need an estimate of the "conventional" part $g_i(\theta)$. We expect this to be of the order of magnitude of the full attenuation in a nonsmectic phase of the same material, since this conventional piece, by construction, only contains short-ranged contributions to the viscosity and hence should not be affected by changes (like smectic layering) which alter only the large-scale symmetry of the system.

¹⁵S. Bhattacharya, S. Y. Shen, and J. B. Ketterson, Phys. Rev. A **19**, 1219 (1979).

¹⁶K. Miyano, Ph.D. Thesis, Northwestern University, 1975 (unpublished).

¹⁷S. Bhattacharya, B. K. Sarma, and J. B. Ketterson, Phys. Rev. Lett. **40**, 1582 (1978); Phys. Rev. B **23**, 2397 (1981).

¹⁸S. Bhattacharya and J. B. Ketterson, Phys. Rev. Lett. **49**, 997 (1982).

¹⁹The parameter a_2 was taken to be zero in Ref. 18 on the advice of the present authors. The resultant a_i 's obeyed (1.3). The success of this fit indicates the relative smallness of the $O(T^2)$ contributions to a_2 compared to the zeroth order in temperature contributions to the other a_i 's.

²⁰The agreement in this case cannot be perfect, of course, since the attenuation in the isotropic phase is, unsurprisingly, isotropic, while in the smectic it is not.

²¹M. Cagnon and G. Durand, Phys. Rev. Lett. **45**, 1418 (1980); J. Phys. Lett. **42**, L451 (1981).

²²M. G. Kim, S. Park, Sr., M. Cooper, and S. V. Letcher, Mol.

- Cryst. Liq. Cryst. **36**, 143 (1976).
- ²³S. Bhattacharya and S. V. Letcher, Phys. Rev. Lett. **44**, 414 (1980).
- ²⁴S. Ramaswamy (unpublished).
- ²⁵D. Forster, *Hydrodynamic Fluctuations, Broken Symmetry, and Correlation Functions* (Benjamin, Reading, Mass., 1975).
- ²⁶Such variables may relax nonhydrodynamically when long-range forces are present. For example electric charge, which is conserved, relaxes at the plasma frequency. Also, the phase of the superconducting order parameter (which is associated with a broken symmetry) relaxes nonhydrodynamically. The long-range force in both of these cases is the Coulomb interaction between electrons. For a fuller discussion of these examples, see Ref. 25.
- ²⁷Strictly speaking, translation invariance in these systems is not broken, due to the Landau-Peierls theorem [A. Caille, C. R. Acad. Sci., Ser. B **274**, 891 (1972); P. G. de Gennes, J. Phys. (Paris) **30**, 9 (1969); Ref. 3, p. 402]; however, this does not affect the correctness of the hydrodynamic description used here.
- ²⁸Displacements along the layers are meaningless since translational invariance is not broken in those directions.
- ²⁹The value Δ chosen in this fashion leads to the result that no term proportional to q_1^2 appears $[\chi^{-1}(\vec{q})]_{uu}$.
- ³⁰This choice of rescaling is, of course, arbitrary, and is made strictly to simplify the recursion relations. Any other choice would give different renormalization-group recursion relations, but the same results for all physical observables.
- ³¹S. Ma and G. Mazenko, Phys. Rev. B **11**, 4077 (1975).
- ³²In this general development the index i , labeling ψ_i , includes a spatial index as well as labeling the type of field and its components. Again a sum over repeated indices is implied.
- ³³Sums over repeated coordinate indices are implied.
- ³⁴The results in Appendix A of Ref. 6 are useful in this analysis.
- ³⁵The reversible, nonfluctuating, nonlinear hydrodynamics of smectics-A has also been considered by H. Brand and H. Pleiner, J. Phys. (Paris) **41**, 553 (1980).
- ³⁶These equations differ slightly from those in I. We believe the present set to be correct; the differences do not affect our results.
- ³⁷Some of this development is discussed in G. F. Mazenko, M. J. Nolan, and R. Freedman, Phys. Rev. B **18**, 2281 (1978).
- ³⁸The bond angle field is included in the dynamics in essentially the same way as for two-dimensional hexatics. For a discussion of the latter, see A. Zippelius, B. I. Halperin, and D. R. Nelson, Phys. Rev. B **22**, 2514 (1980); A. Zippelius, Phys. Rev. A **22**, 732 (1980).
- ³⁹Some terms in the Fourier transform of (4.1) are irrelevant when computing the divergent contributions to the viscosities; we neglect these terms in (4.5).
- ⁴⁰This term arises from the $(\nabla_i u)\delta F/\delta u$ term in the equation of motion for g_i , when one considers the $(\vec{\nabla} u)^4$ term in F .
- ⁴¹Such six-point and higher vertices do not exist in the precise dynamical model we are considering. They would, however, arise if higher (even) powers of the invariant $E \equiv \vec{\nabla}_z u - \frac{1}{2} |\vec{\nabla} u|^2$ were included in the free energy. Such irrelevant terms are presumably present in any real smectic free energy; furthermore, even if our initial model does not contain them, they will be generated by the static renormalization group of Sec. II.
- ⁴²As seen, for example, in Fig. 6(c) on the left-side vertex.
- ⁴³It should be emphasized that this renormalized vertex has nothing whatsoever to do with the form of the terms quadratic in u in the equation of motion for g . The latter is always given by $[B_R(\vec{q})\delta_{iz}\delta_{jz} - C_R(\vec{q})\delta_{ij}]q_j p^2$ while the former, as we shall see, involves further adjustable parameters and has a more general tensor structure.
- ⁴⁴It might seem possible at this point that a more divergent graph could be made by inserting the smaller $u-\vec{g}_1$ propagator, and compensating for its smallness by the larger \vec{g}_1-u-u vertex. It is not.
- ⁴⁵The origin of the factor C_H lies in higher-order graphs of the type shown in Figure 8, all of which, like the one-loop graph, diverge like $1/H^2$ as $H \rightarrow 0$, but which are higher order in temperature. We have only explicitly evaluated the one-loop graph, and then lumped our ignorance of these higher-order graphs (see Fig. 9) into the factor $C_H(T)$, which contributes the same overall multiplicative factor to all four divergent viscosities; and furthermore clearly approaches unity as $T \rightarrow 0$, since the higher-order graphs become negligible in that limit.